Coherent imaging by near and far-field diffraction

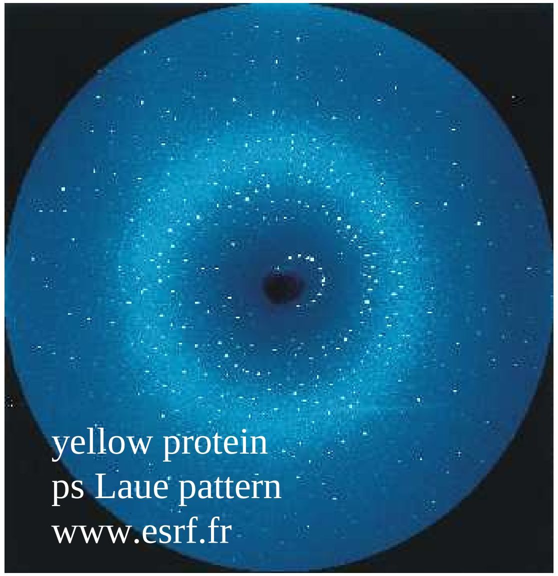

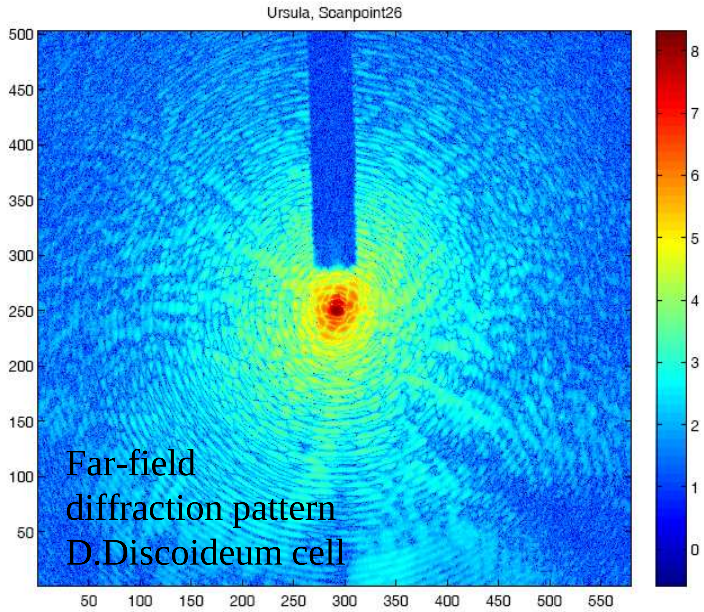

1. ***Why x-ray imaging ?***
2. ***The phase problem***
3. ***How to: the far-field (CDI)***
4. ***How to: the near-field (propagation imaging)***
5. ***From synchrotron to FEL***

Tim Salditt, Institut für Röntgenphysik
Universität Göttingen, UXSS 2011

SFB 755

Imaging with x-rays- advantage No.1: transparency

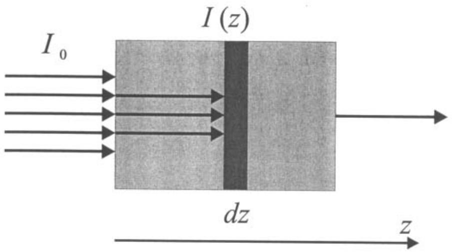

$$I(z) = I_0 e^{-\mu z}$$

absorption coefficient $\mu \sim E^{-3} \quad Z^{-4}$

look into biomaterials

(bulk information)

X-ray advantage No.2:
(a) quantitative contrast and weak scattering cross section

index $n = 1 - \delta + i\,\beta$, $\delta, \beta \approx 10^{-5}$-$10^{-6}$
close to 1.
$\Rightarrow$ reduced reflections at internal interfaces

no multiple scattering

(look through foam of beer, R.W. Pohl 1939)

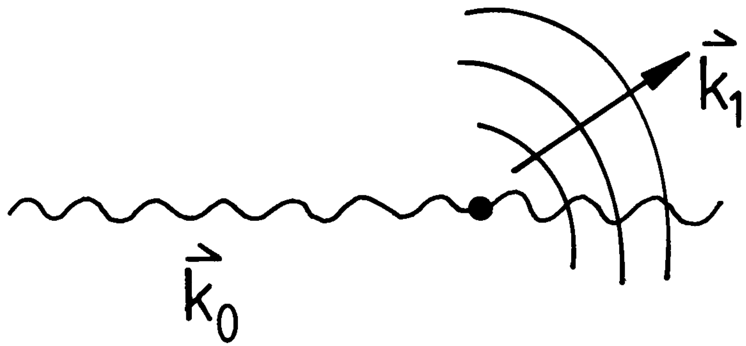

$$e^{i\vec{k}_0\cdot\vec{r}} \longrightarrow e^{i\vec{k}_0\cdot\vec{r}} + f(\Omega)\,\frac{e^{ik_0\cdot r}}{r}$$

$f(\Omega)$ amplitude, $[f(\Omega)] = m$ „scattering length "
$f = 2.82\ 10^{-15}$ m

(Born Approx.)

advantage No.3: small wavelength – high resolution

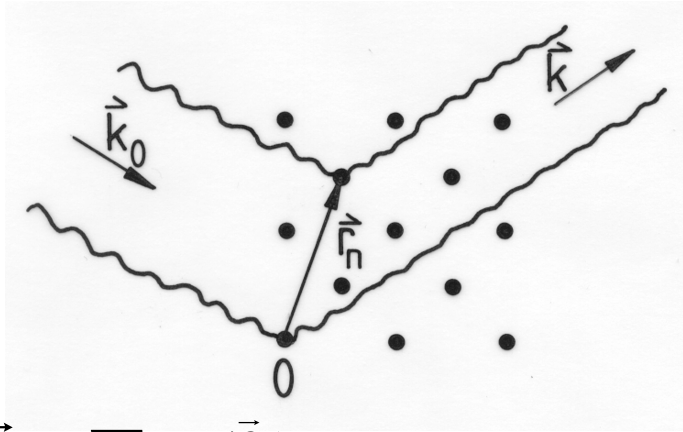

$$S(\vec{Q}) = \sum_n f_n e^{i\vec{Q}\cdot\vec{r}_n}$$

X-ray nobel prizes:
Laue, Bragg, Debey, Perutz&Kendrew, Hodgkin, Watson&Crick,
Deisenhofer, Huber & Michel, Agre, McKinnon,
And many more (> 25 scientists !)

Laue 1912

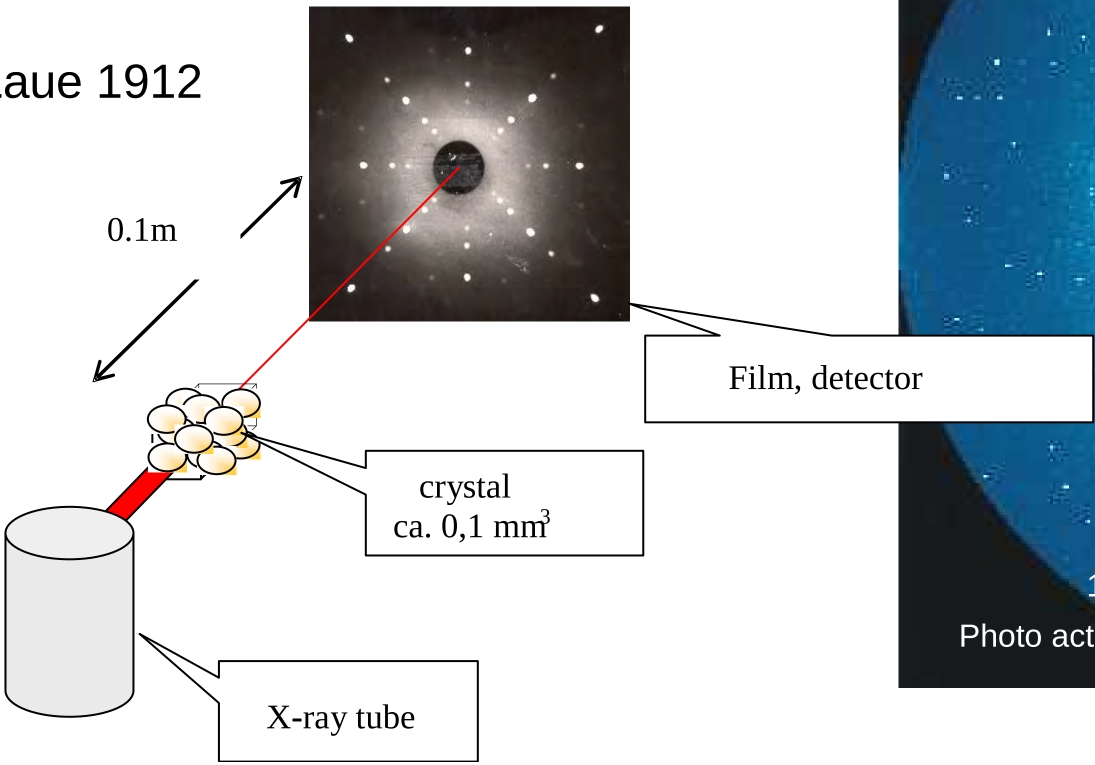

electron density !

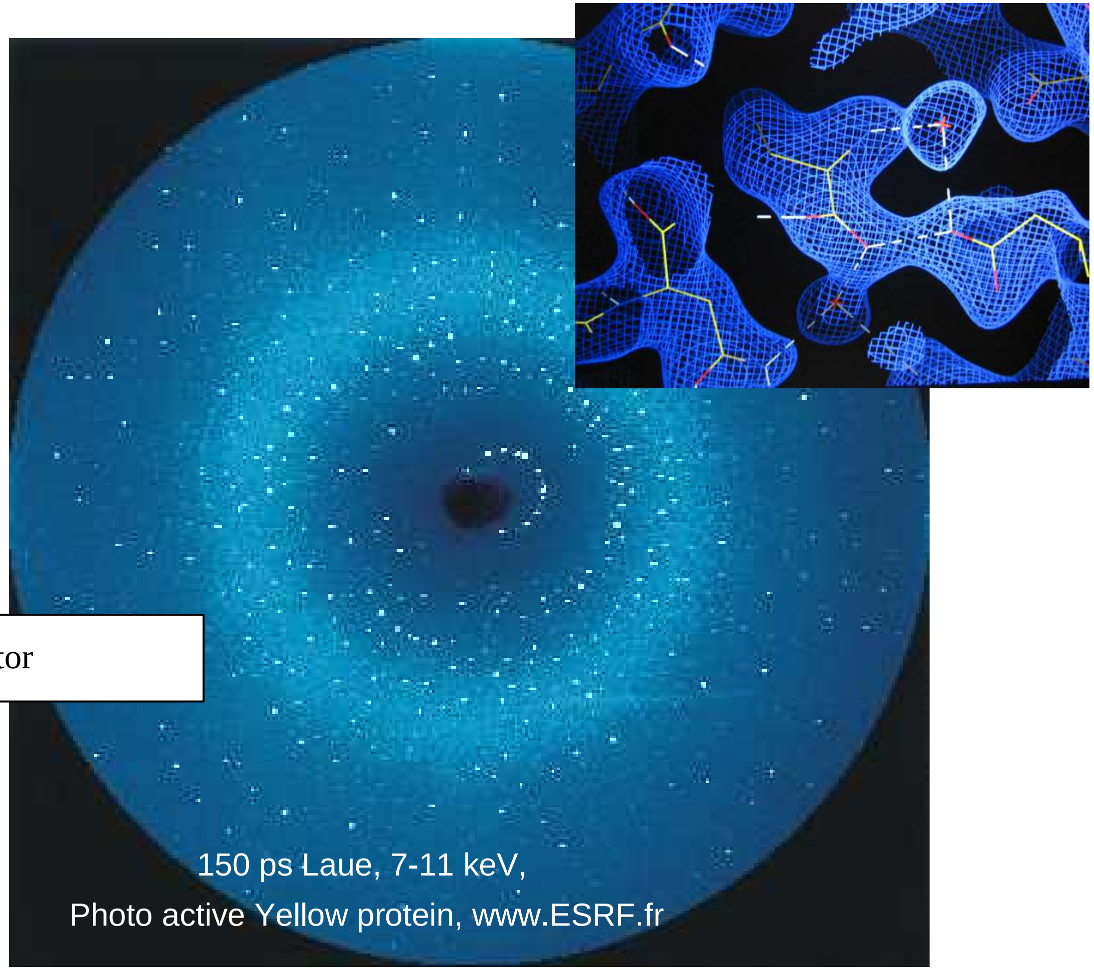

4th advantage: short pulses -- the spatio-temporal map

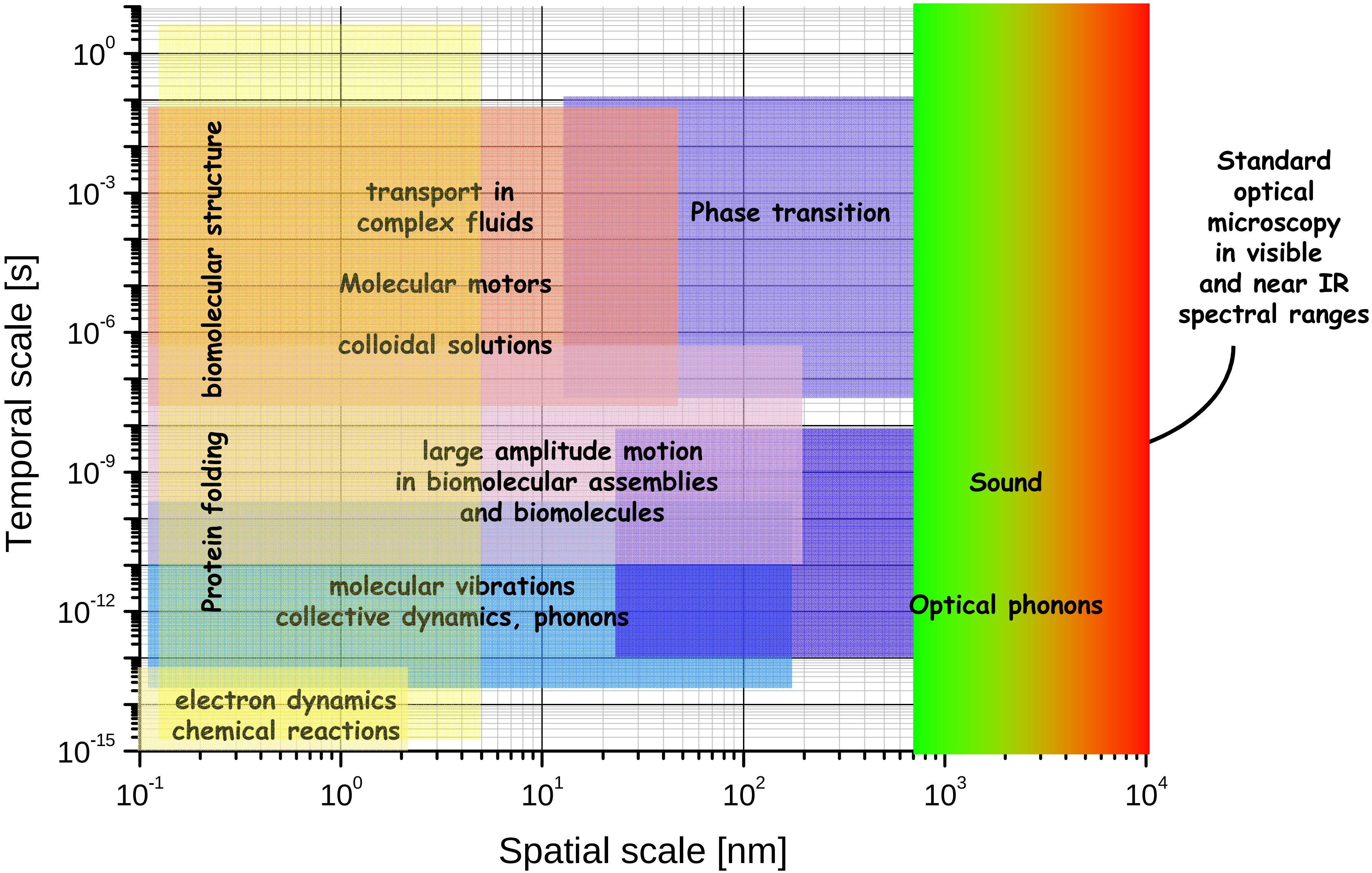

$$\Delta x \approx \frac{\lambda}{2n \sin \alpha}$$

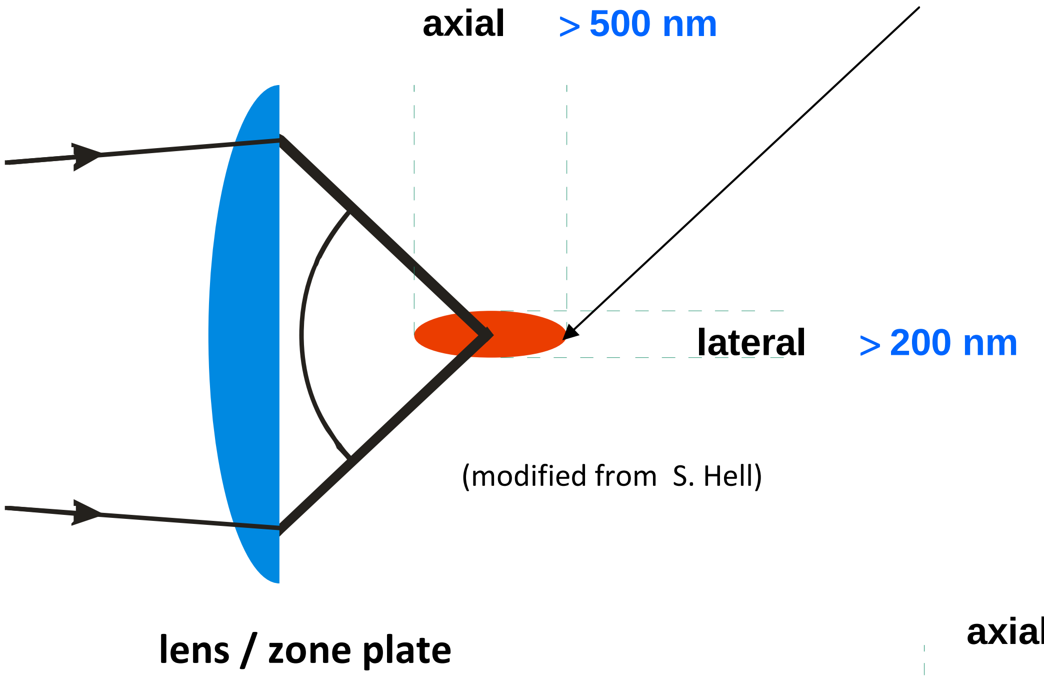

Conventional
light microscopy
is limited by diffraction.

Conventional
X-ray microscopy
is limited by diffraction
Structures.

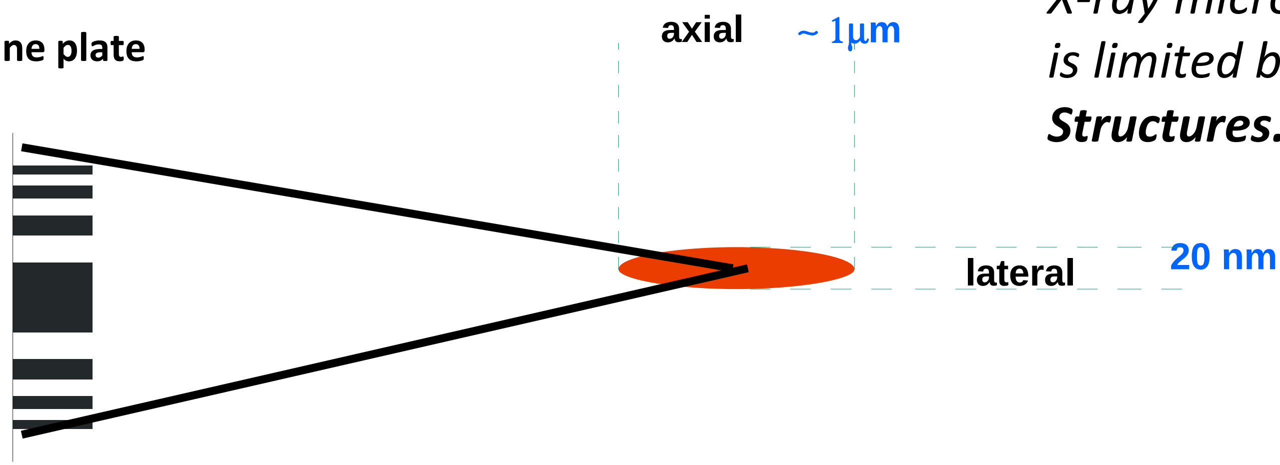

Fresnel Zone Plate (FZP) based x-ray microscopy

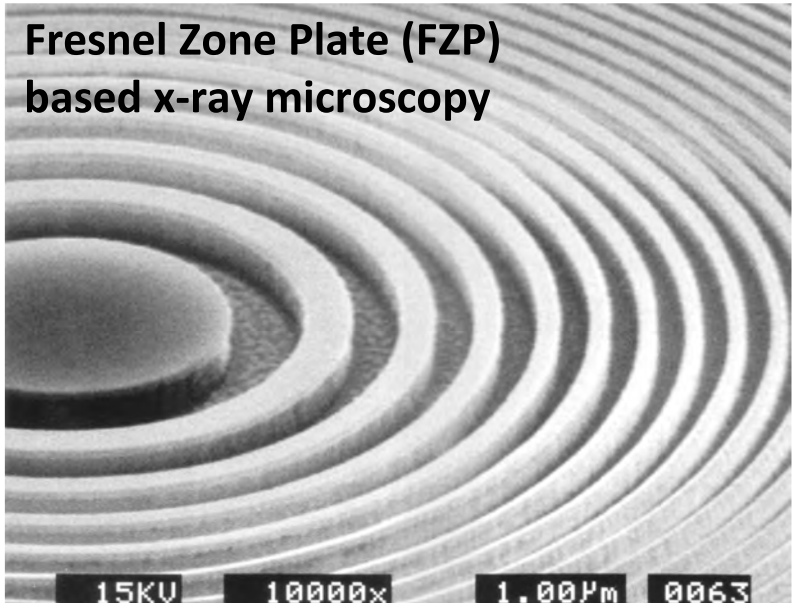

G. Schmahl, D. Rudolph, Univ. Göttingen

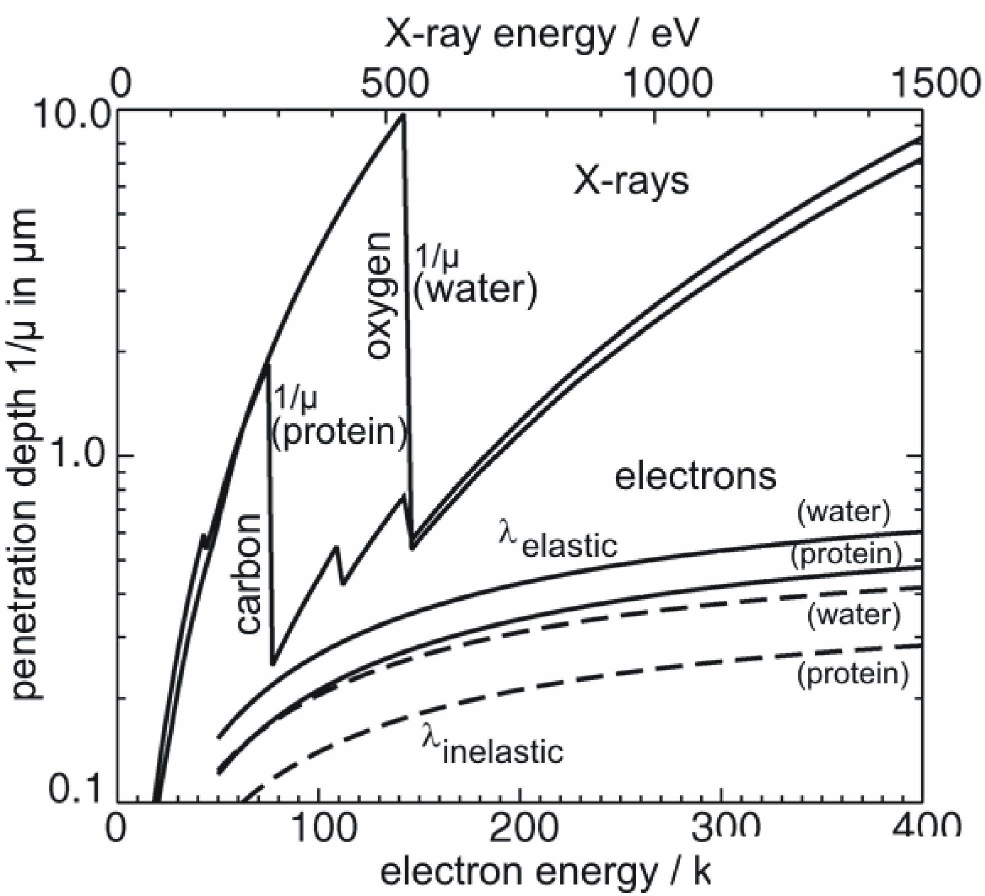

from J. Kirz et al.

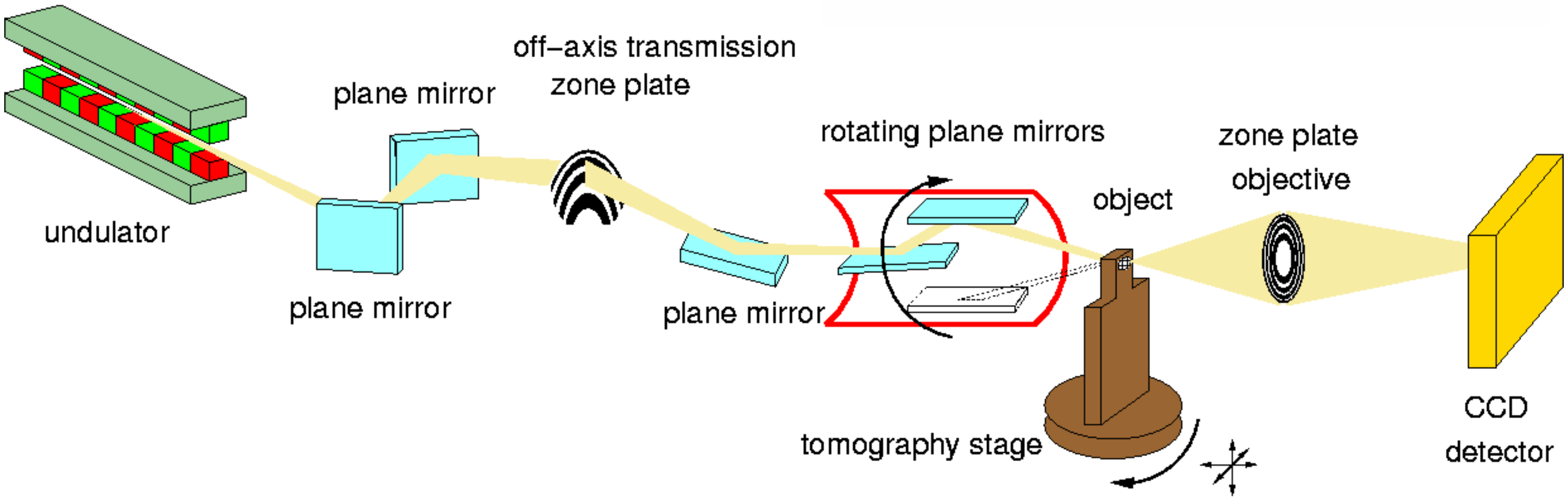

Interference of two point scattering centers

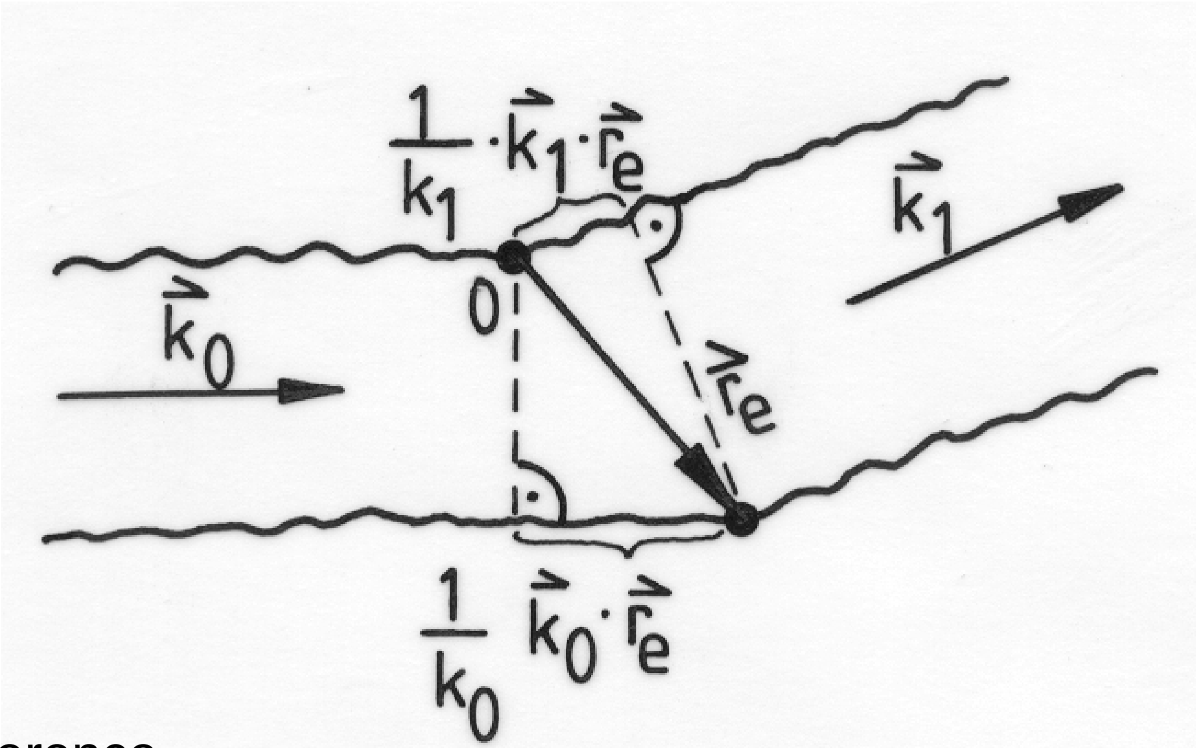

Phase difference

$$= \frac{2\pi}{\lambda_0} \text{ opt.Weg} = \frac{2\pi}{\lambda_0} \; \frac{1}{k_0} \; \left(\vec{k}_0 - \vec{k}_1\right) = \left(\vec{k}_0 - \vec{k}_1\right) \cdot \vec{r}_e = \vec{q} \cdot \vec{r}$$

elastic $\qquad k_0 = k_1$

Interference: from two points to a crystal …

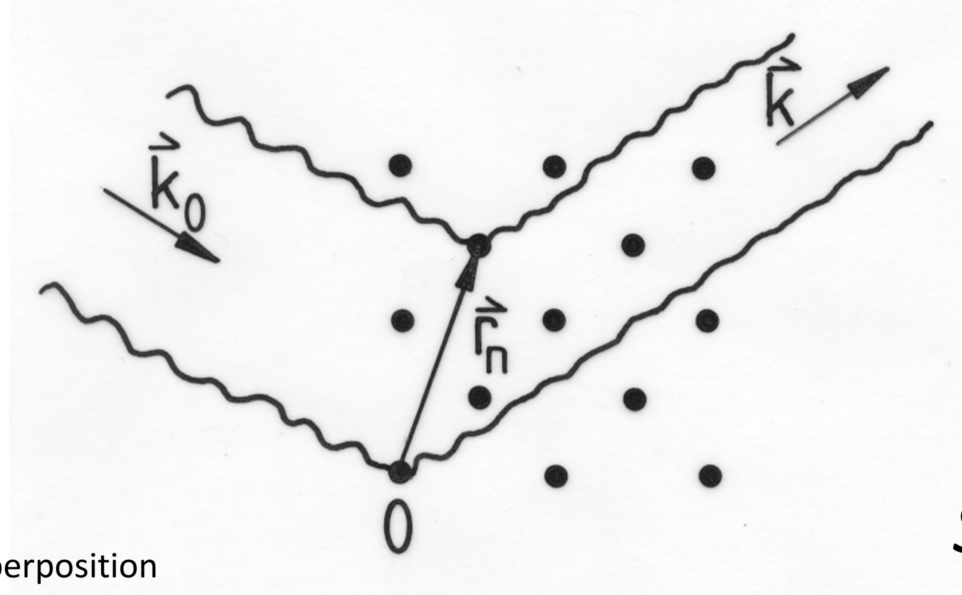

Atoms (Molecules) on a lattice :

$$\vec{r}_n = n_1\vec{a} + n_2\vec{b} + n_3\vec{c} \qquad n_i = 1,2,3\ldots$$

simplification: $f_n = f$

$$S(\vec{q}) = \sum_n f_n e^{i\vec{q}\cdot\vec{r}_n}$$

Superposition
In the far-field

$$S(\vec{q}) = \sum_n^N e^{i\vec{q}\cdot\vec{r}_n} = \sum_{n_1 n_2 n_3}^N e^{i\vec{q}\cdot\left(n_1\vec{a}+n_2\vec{b}+n_3\vec{c}\right)} = \left(\sum_{n_1}^{N_1} e^{in_1\vec{q}\cdot\vec{a}}\right)\left(\sum_{n_2}^{N_2} e^{in_2\vec{q}\cdot\vec{b}}\right)\left(\sum_{n_3}^{N_3} e^{in_3\vec{q}\cdot\vec{c}}\right)$$

$$\sum_{n_1}^{N} e^{in_1\vec{q}\cdot\vec{a}} = \frac{\sin\frac{N_1}{2}\left(\vec{q}\cdot\vec{a}\right)}{\sin\frac{1}{2}\left(\vec{q}\cdot\vec{a}\right)}$$

$$\vec{q}\cdot\vec{a} = 2\pi q$$
$$\vec{q}\cdot\vec{b} = 2\pi r$$
$$\vec{q}\cdot\vec{c} = 2\pi s$$

Continuous electron densities:
the form factor

$$\sum_m e^{i\vec{q}\cdot\vec{r}_m} \rightarrow \int_V d^3r\ n_e(\vec{r})\ e^{i\vec{q}\cdot\vec{r}_m} = f\left(\vec{q}\right)$$

CDI : a simple far-field diffraction experiment

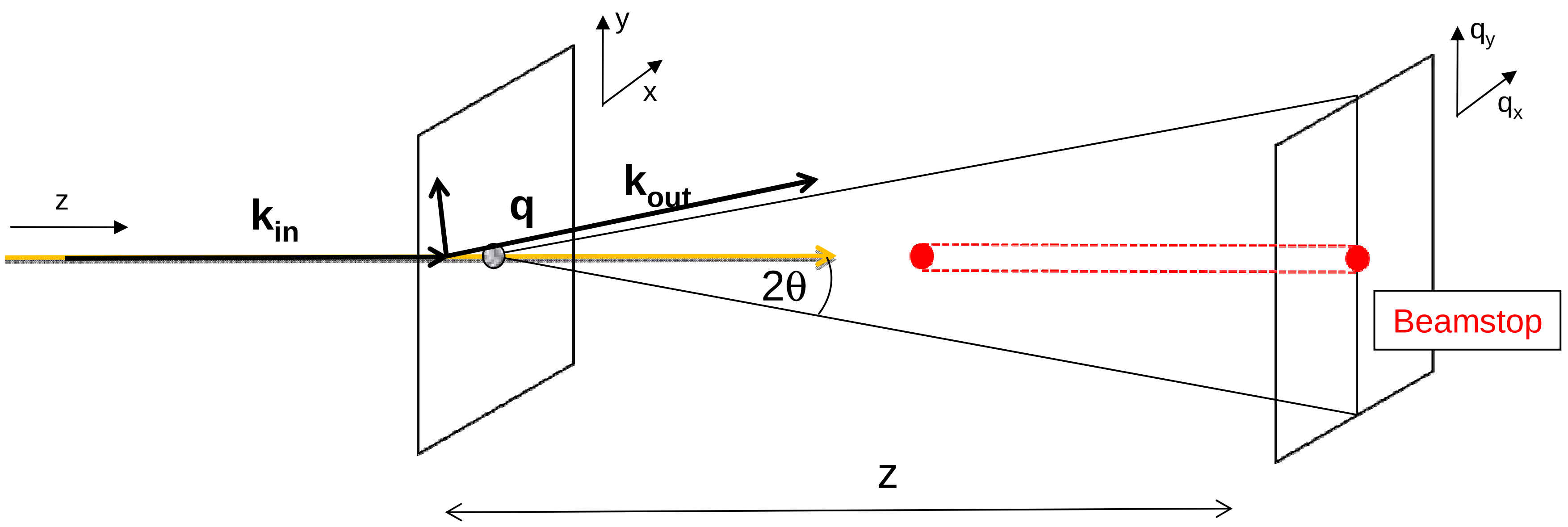

Object Scattering potential

$$o(\vec{x}) = r_e \rho(\vec{x}) = \frac{\pi}{\lambda^2}\left(1 - n^2(\vec{x})\right)$$

$$\approx \frac{2\pi}{\lambda^2}\left(\delta(\vec{x}) + \mathrm{i}\beta(\vec{x})\right)$$

$$= \frac{2\pi}{\lambda^2}\Delta n(\vec{x})$$

Observed intensity at Fraunhofer plane

$$I(\overline{q}) \propto I_0 \cdot \left|O(\overline{q})\right|^2$$

$$= I_0 \cdot \left|\int P_z\left[o(\vec{x})\right]\exp(2\pi\,\mathrm{i}\cdot\overline{\mathrm{q}}\cdot\overline{\mathrm{x}})\;\mathrm{d}\overline{\mathrm{x}}\right|^2$$

as Born and projection approximation valid ...

with

$$o(\overline{x} = (x, y)) = P_z\left[o(\vec{x} = (x, y, z))\right] = \int o(x, y, z)\;\mathrm{d}z$$

Lenseless (diffractive) imaging with coherent x-rays

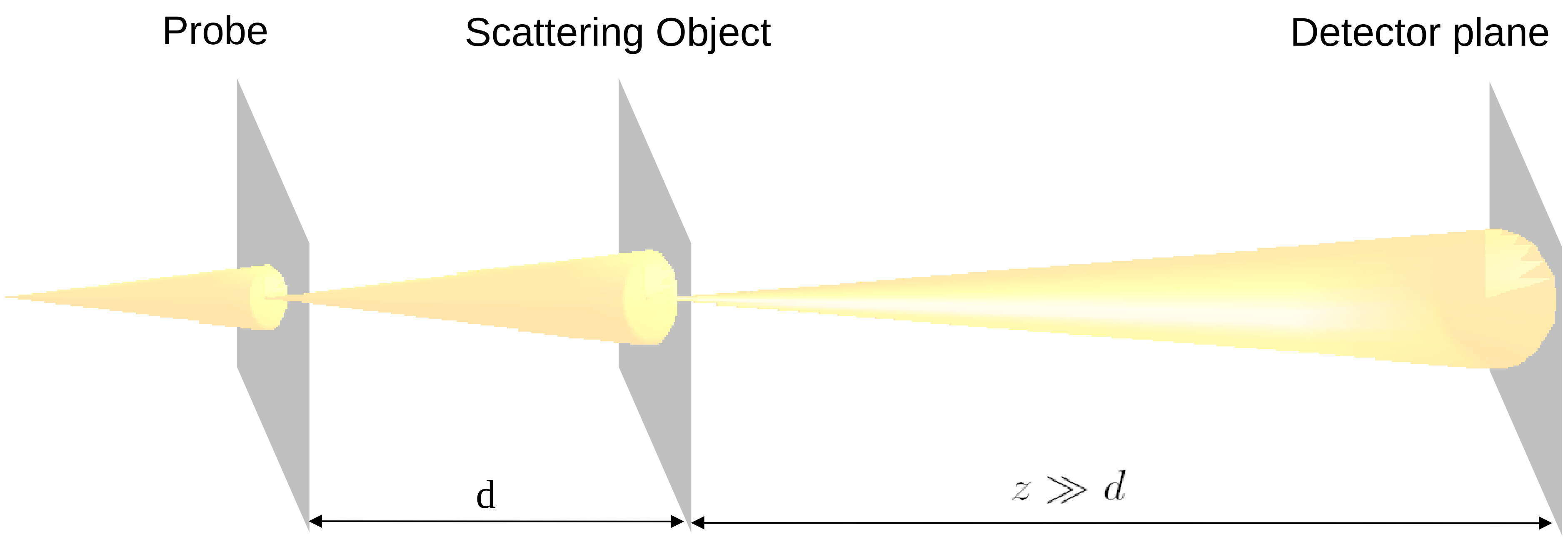

$P(\mathbf{r})$ $\quad\quad$ $\Psi(\mathbf{r}) = P(\mathbf{r} + (0,0,d)) \cdot O(\mathbf{r})$ $\quad\quad$ $|\mathcal{F}(\Psi)|^2 = |\mathcal{F}(P_d) \times \mathcal{F}(O)|^2$

- projection approximation, multiplicity of P and O
- measured intensity is given as a convolution of object and probe function
- transversal coherence length must be larger than sample
- Use iterative algorithm to retrieve O from its modulus squared Fourier transform
- Separate P and O either experimentally or theoretically

The phase problem

Augustin Jean Fresnel, 1788-1827

Wilhelm Conrad Röntgen, 1845-1923

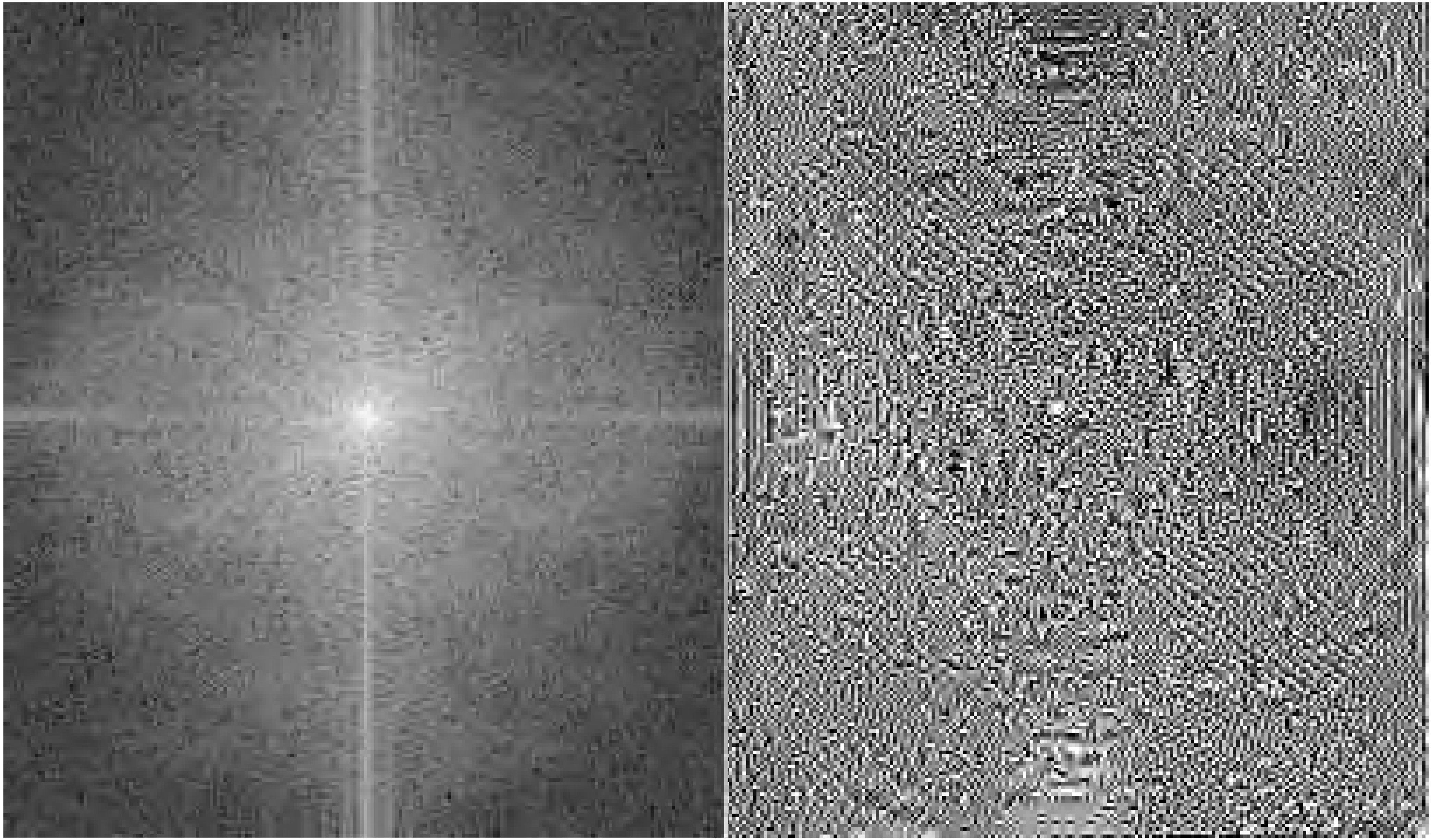

$$\hat{\rho}_{\mathrm{kl}} = \frac{1}{\sqrt{N \cdot M}} \sum_{i=0}^{N-1} \sum_{j=0}^{M-1} \rho_{ij}\, e^{-2\pi i \left(\frac{ik}{N} + \frac{jl}{M}\right)}$$


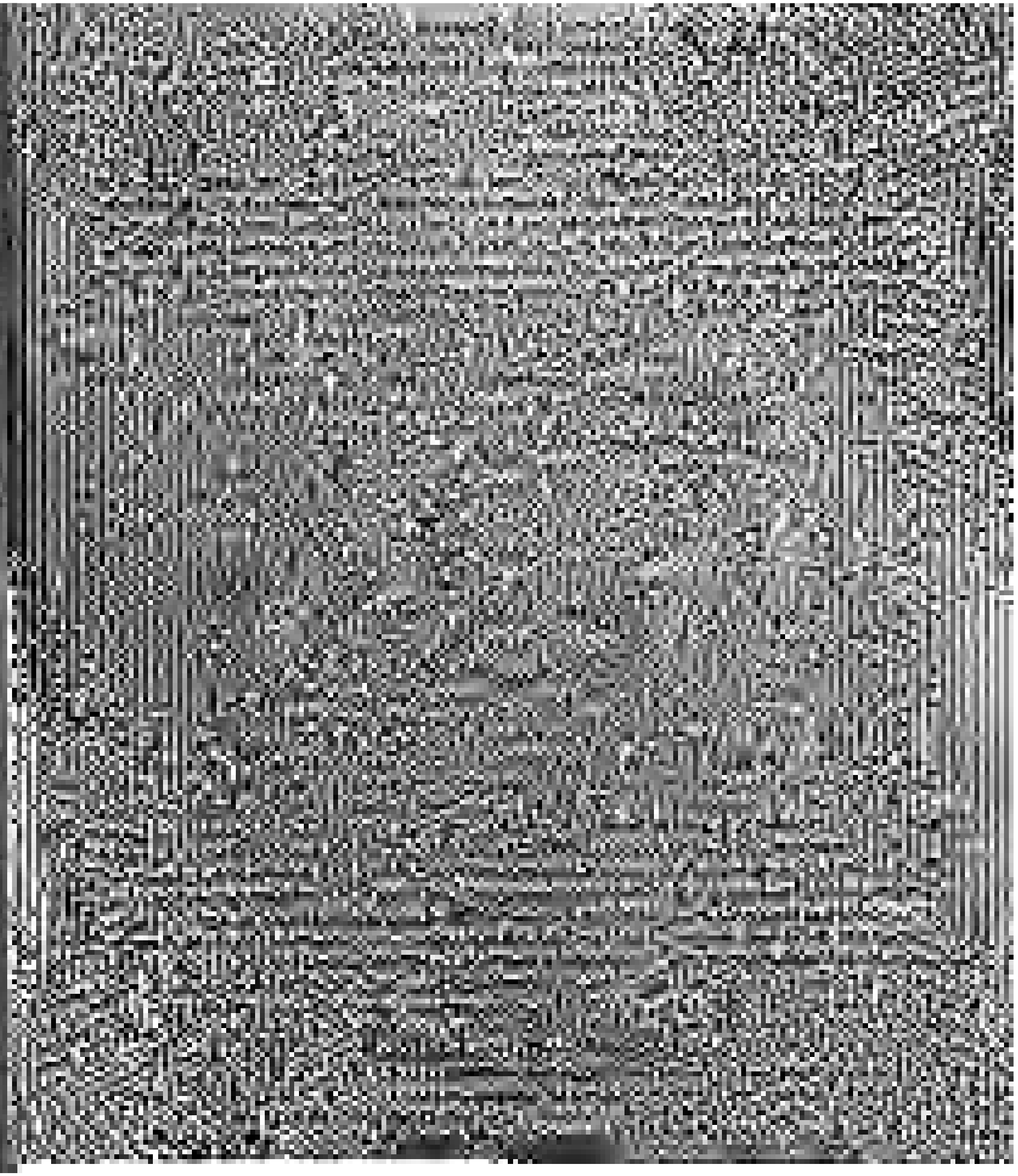


Phase Problem

Problem

$$\int o(\overline{x})\exp(2\pi \mathrm{i}\cdot\overline{\mathrm{q}}\cdot\overline{\mathrm{x}})\,\mathrm{d}\overline{\mathrm{x}} \in \mathrm{C} \qquad \text{but} \qquad I(\overline{q}) \propto I_0 \cdot \left|\int o(\overline{x})\exp(2\pi \mathrm{i}\cdot\overline{\mathrm{q}}\cdot\overline{\mathrm{x}})\,\mathrm{d}\overline{\mathrm{x}}\right|^2 \in \mathrm{R}$$

„Half“ of the information, **the phase** is lost!

How to get $o(\overline{x}) = e\rho(\overline{x})$ then ?

Real data: problem is discretized:

$$I(q_x^{(k)}, q_y^{(l)}) = \left|\sum_{i,j=1}^{N} o(x_i, y_j)\exp\left(2\pi \mathrm{i}\cdot\frac{q_x^{(k)}\cdot \mathrm{x_i} + q_y^{(l)}\cdot \mathrm{y_j}}{N}\right)\right|^2$$

$$= \sum_{\overline{x},\overline{x}'} c_{\overline{x},\overline{x}'}(\overline{q})\; o(\overline{x})\cdot o^*(\overline{x}')$$

with

$$x_j = j\Delta x;\;\; j = 1..N$$
$$y_j = j\Delta y;\;\; j = 1..N$$
$$q_{x,y}^{(j)} = j\Delta q;\;\; j = 1..N$$

Is there a way to reconstruct o(x,y) from I(q) from this nonlinear system of equations?

„Oversampling“: a strategy to render the problem unique ?

real space $\left|\mathcal{F}\right|$ **reciprocal space**

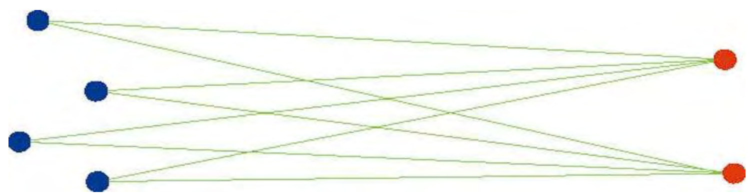

$$I(\vec{q}) \propto \left| \sum_{i,j} \rho_{ij} e^{i\vec{q}\cdot\vec{r}_i} \right|^2$$

“Oversampling”

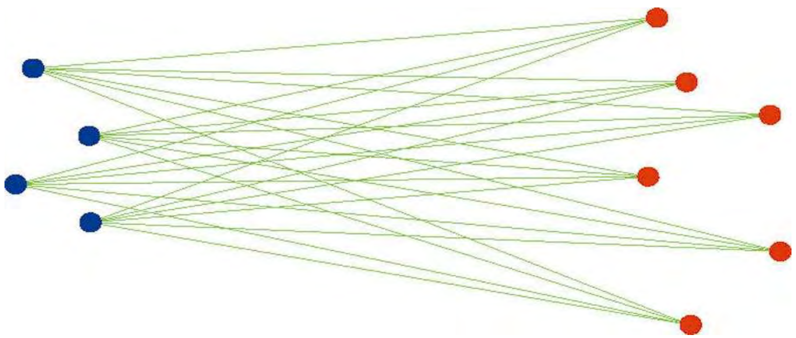

Information theory (Shannon) ?
really more information

J.Miao et al., *J. Opt. Soc. Am*. ’98
J.Fienup, *Appl. Opt.* 21, 2758 (1982)
J.Miao, J. Kirz & D. Sayre, *Acta Cryst*. D 56, 1312 (2000)

More unknowns than equations ?

$$\mathrm{I}(\mathrm{q}_{\mathrm{kl}}) = \mathrm{F}(\mathrm{q}_{\mathrm{kl}})\,\mathrm{F}^*(q_{kl}) = \left|\sum_i^{N-1}\sum_j^{N-1}\rho_{ij}\; e^{-i(q_k\, x_i + q_l\, y_i)}\right|^2 \qquad h,k,i,j = 0\ldots N-1$$

N^2 (2D) unknowns ρ_{ij},
but only $N^2/2$ independent equations

$$F(q) = F^*(-q)$$

$\rho(r)$ =0 out of support !

If support is half the size of
the field of view in both both dimensions:

N^2 (2D) unknowns ρ_{ij},
4 N^2 equations
2 N^2 independent equations

But how to solve this set of independent equations ?

Fienup 1978, Miao 1999, Elser 2000-

Solution of the phase probelm by iterative algorithms

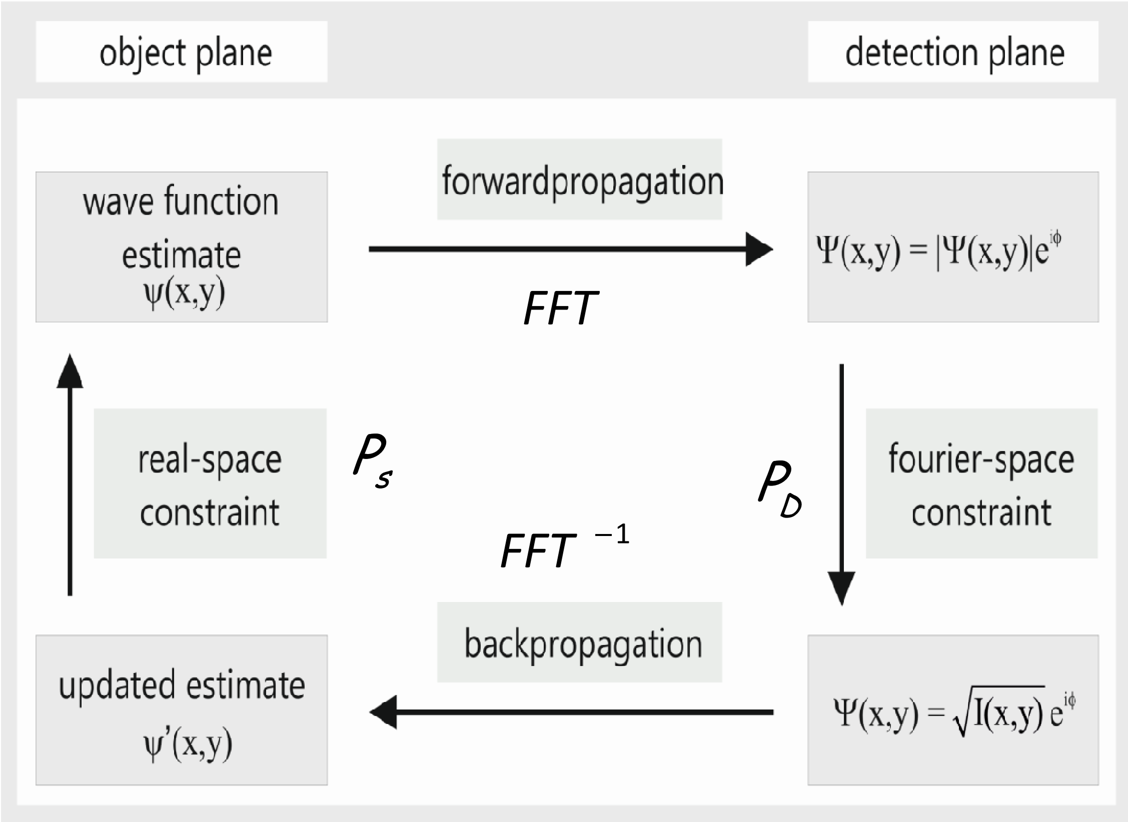

$$\rho_{i+1}(r) =$$

$$\begin{cases} \rho_i'(r) & r \in S \cap \rho_i'(r) > 0 \\ \rho_i(r) - \beta\, \rho_i'(r) & r \notin S \cup \rho_i' \leq 0 \end{cases}$$

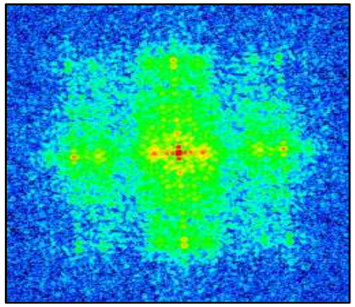

coherent scattering patte

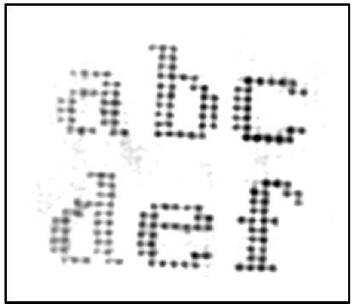

reconstructed image

*J. Miao et al., Nature **400**, 342 (1999)*

PRL 102, 018101 (2009) PHYSICAL REVIEW LETTERS week ending 9 JANUARY 2009

Three-Dimensional Visualization of a Human Chromosome Using Coherent X-Ray Diffraction

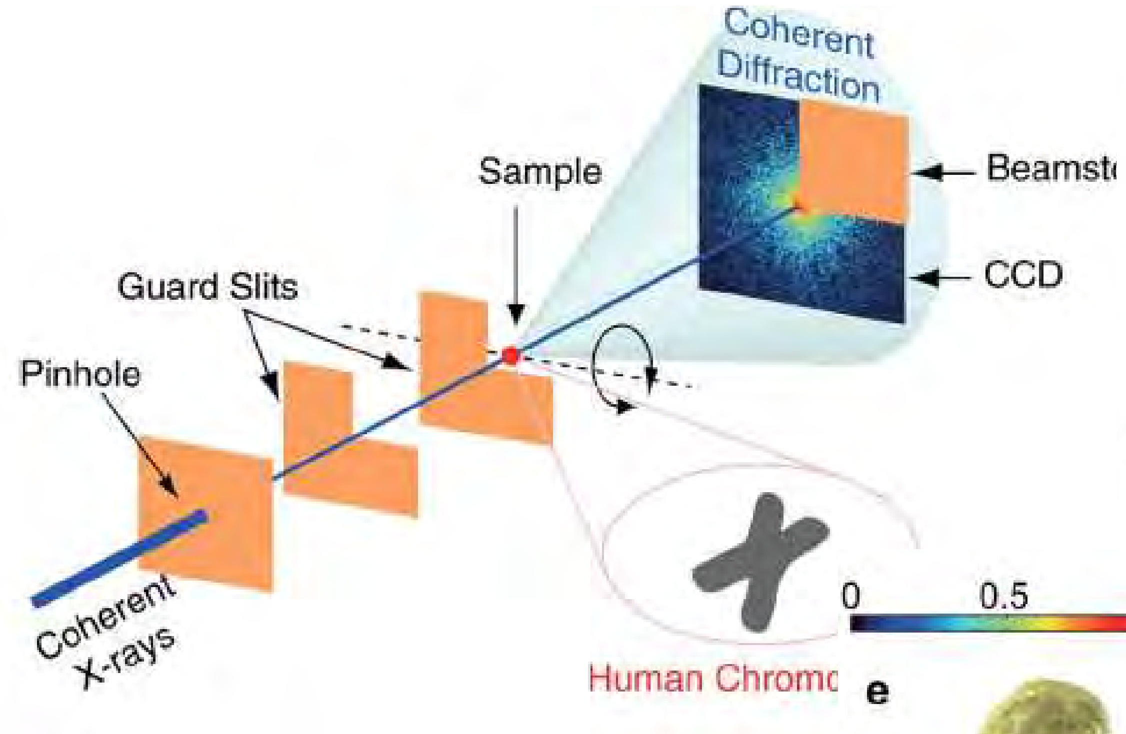

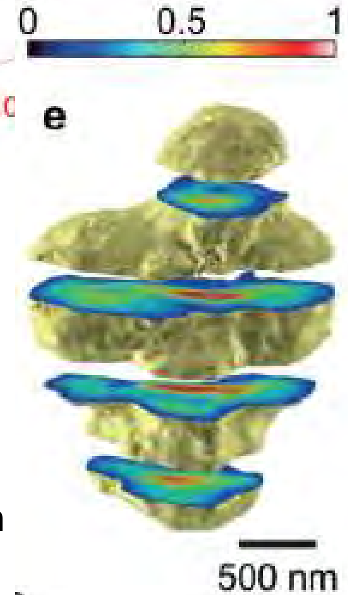

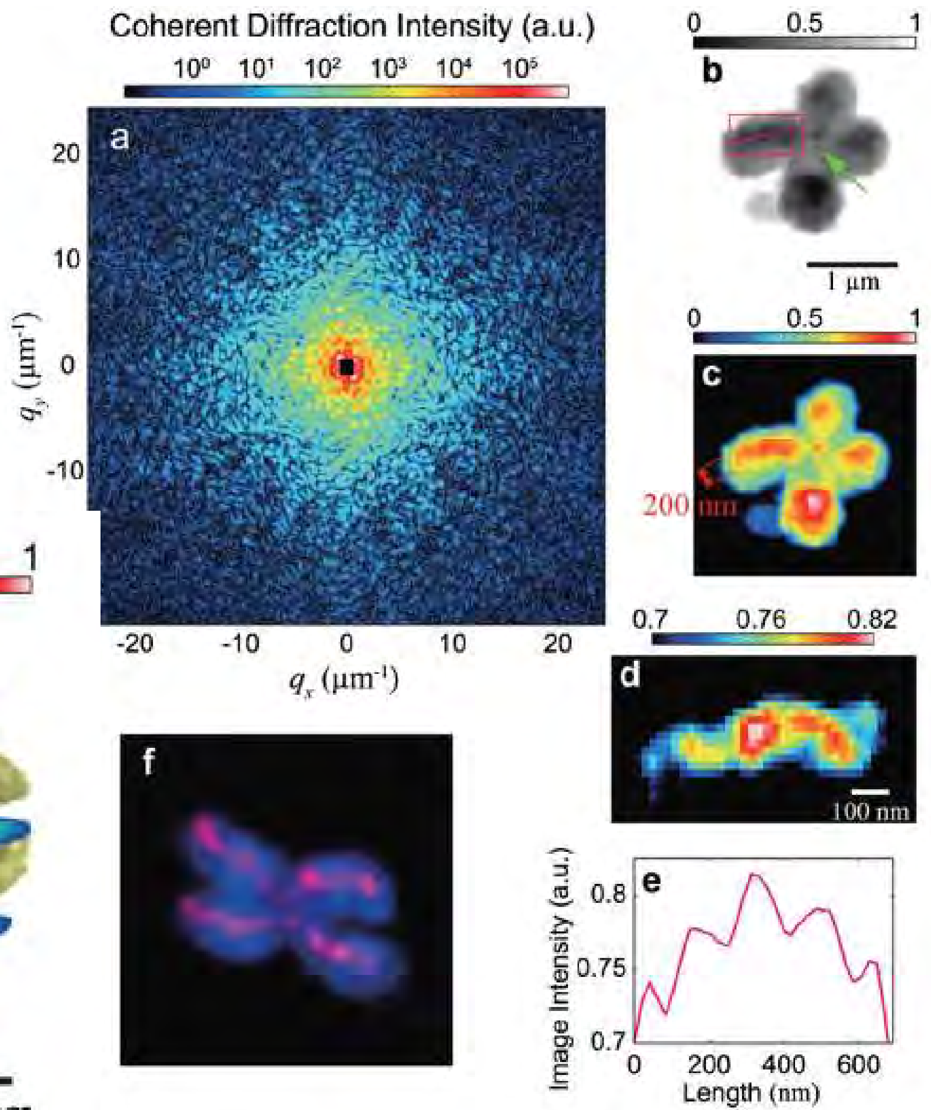

freeze dried Chromosomes from HELA cells
Flux: 10^{10} cps in 33µm (5 keV)
accumulation time: 2700s per projection
56 projections
resolution of 2D projection image: ~ 30nm
resolution of the 3D reconstruction: ~ 120 nm
radiation dose (tomography) : 2 10^{10} Gy
results: chromatin, heterochromatin in centromere

FIG. 2 (color). Coherent diffraction pattern of an unstained human chromosome and its reconstructed projection image. The

The Mimi virus: single shot biological imaging with an FEL

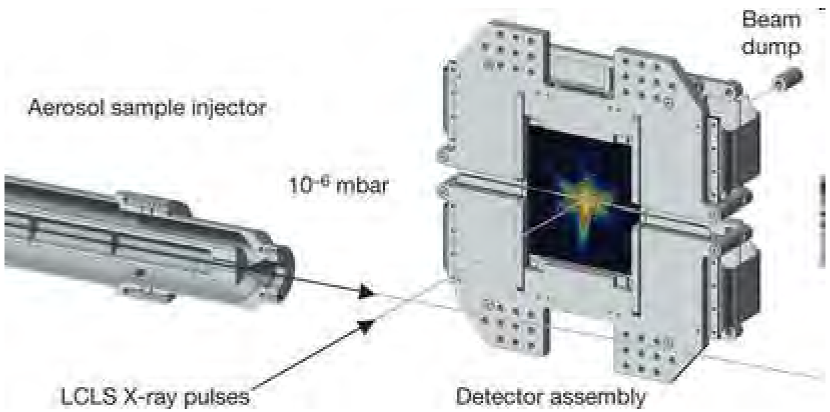

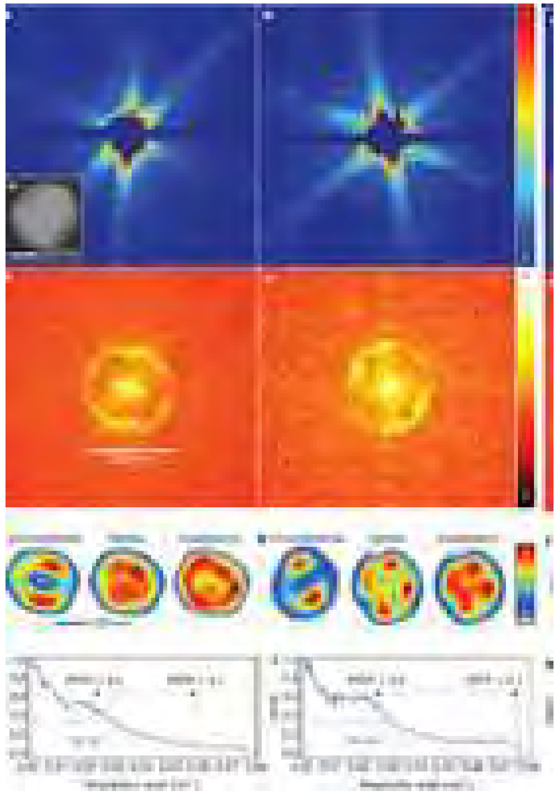

Nature | Letter

Single mimivirus particles intercepted and imaged with an X-ray laser
Seibert et al. (2011)

LCLS, Haidu Chapman collaborations

outlook:Single particle (molecule) crystallography

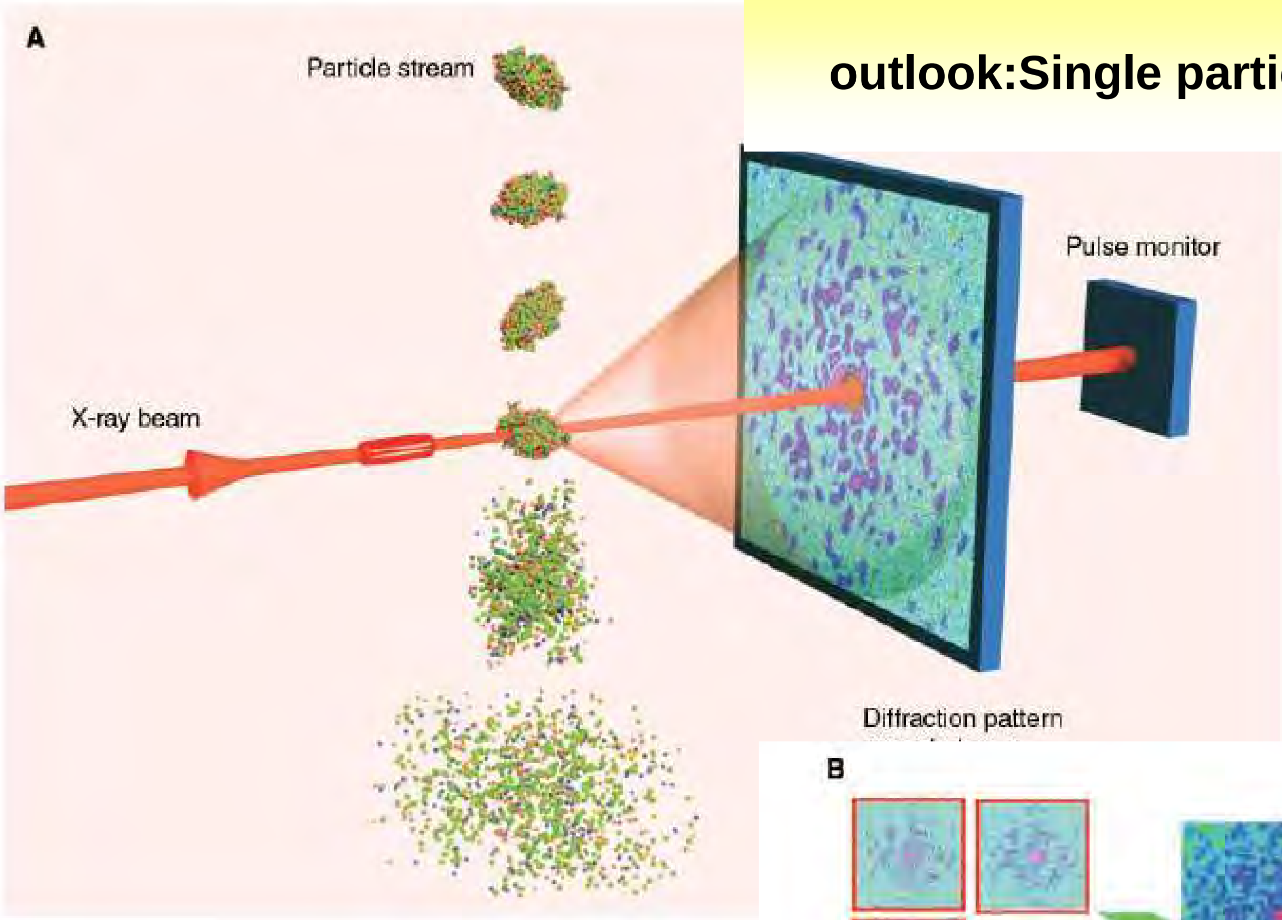

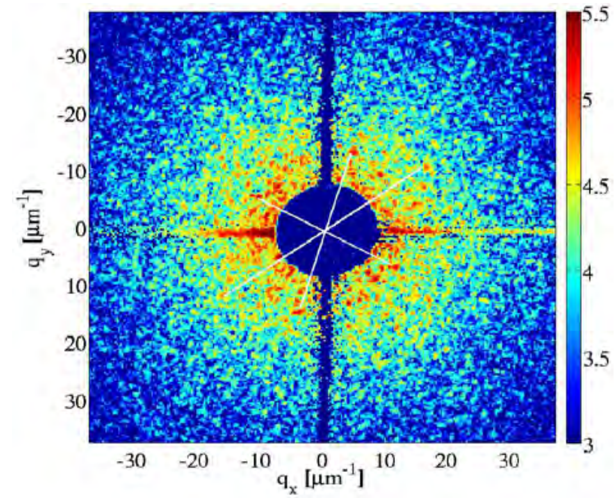

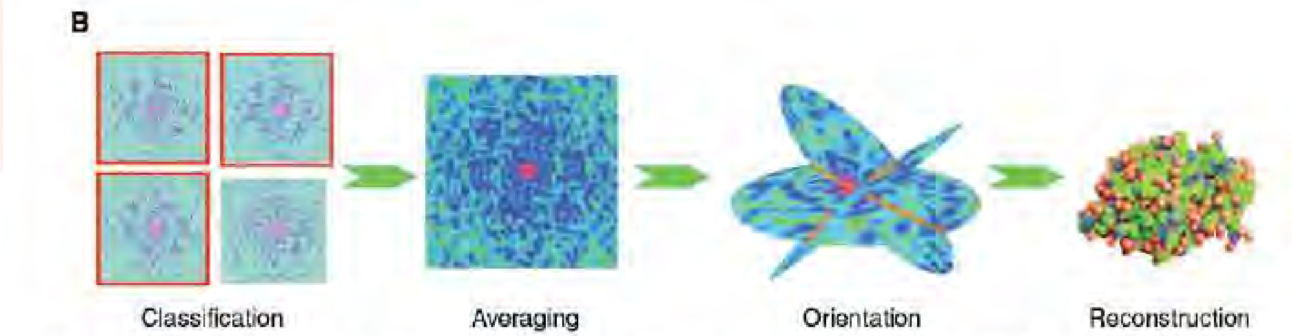

Imaging Atomic Structure and Dynamics with Ultrafast X-ray Scattering
K. J. Gaffney, *et al.*
Science **316**, 1444 (2007);

Fig. 2. Schematic depiction of single-particle coherent diffractive imaging with an XFEL pulse. (**A**) The intensity pattern formed from the intense x-ray pulse (incident from left) scattering off the object is recorded on a pixellated detector. The pulse also photo-ionizes the sample. This leads to plasma formation and Coulomb explosion of the highly ionized particle, so only one diffraction pattern [a single two-dimensional (2D) view] can be recorded from the particle. Many individual diffraction patterns are recorded from single particles in a jet (traveling from top to bottom). The particles travel fast enough to clear the beam by the time the next pulse (and particle) arrives. The data must be read out from the detector just as quickly. (**B**) The full 3D diffraction data set is assembled from noisy diffraction patterns of identical particles in random and unknown orientations. Patterns are classified to group patterns of like orientation, averaged within the groups to increase signal to noise, oriented with respect to one another, and combined into a 3D reciprocal space. The image is then obtained by phase retrieval.

Ptychography Technique

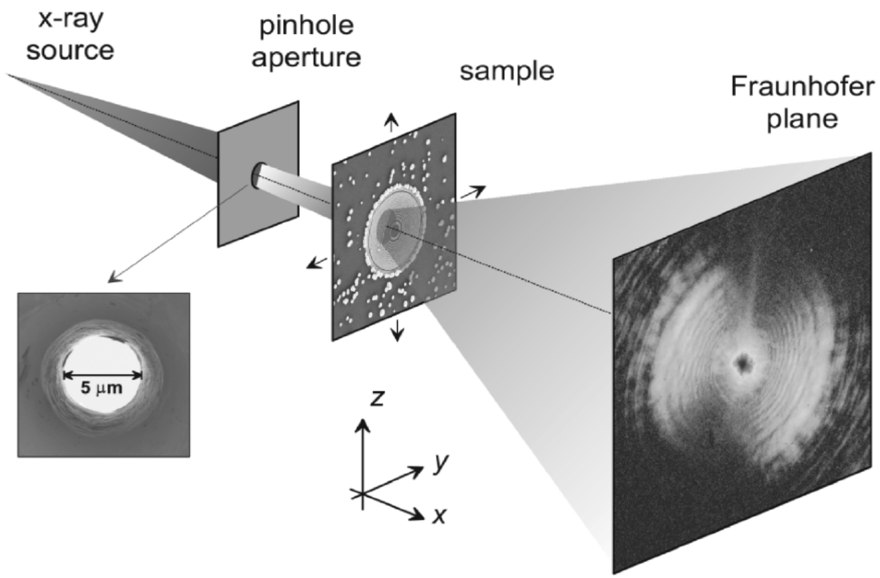

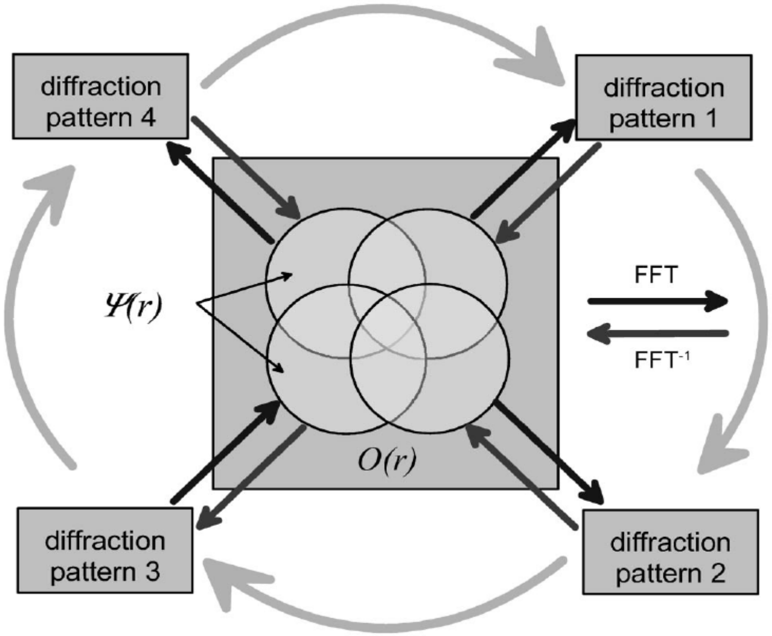

Rodenburg *et al. PRL* **98**, 034801 (2007)

Without probe retrieval: Ptychographic Iterative Engine (PIE)

Nellist, P.D., McCallum, B.C. and Rodenburg, J.M. *Nature* **374**, 630 (1995)
Rodenburg *et al. PRL* **98**, 034801 (2007)

With probe retrieval: Scanning X-ray Diffraction Microscopy or Ptychographic CDI

Thibault, P. *et al. Science* **321**, 379 (2008)
Guizar-Sicairos M., and Fienup, J.R. *Optics Express* **16**, 94330 (2008)

reconstruction of object and illumination function

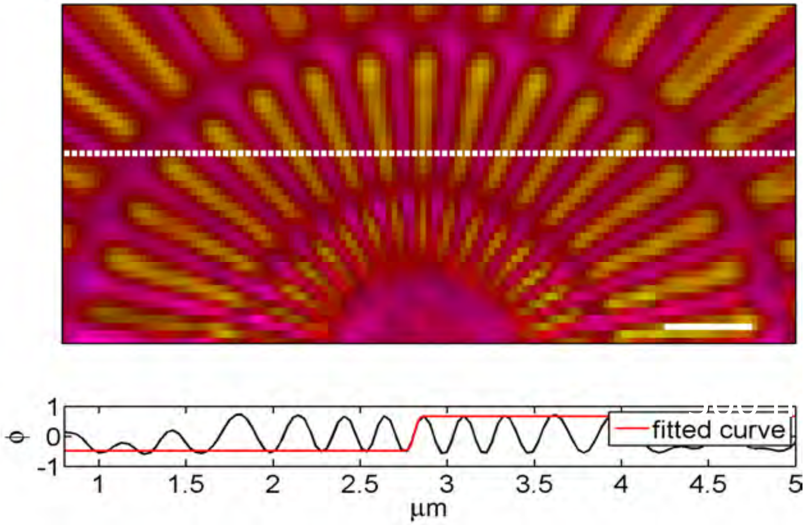

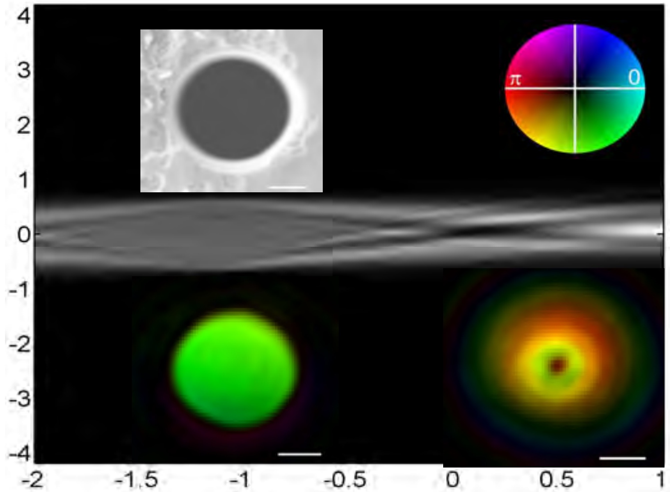

Giewekemeyer *et al.*, PNAS (2010)

6.2 keV 500 nm Ta test sample Resolution (FWHM) 50 nm, fluence $5.1 \cdot 10^6$ ph/µm^2
Measured phase and amplitude change: 0.34p and 0.86 (expected: 0.34p and 0.88)

$$\Psi(\mathbf{r}) = P(\mathbf{r} + (0,0,d)) \cdot O(\mathbf{r}) \qquad |\mathcal{F}(\Psi)|^2 = |\mathcal{F}(P_d) \times \mathcal{F}(O)|^2$$

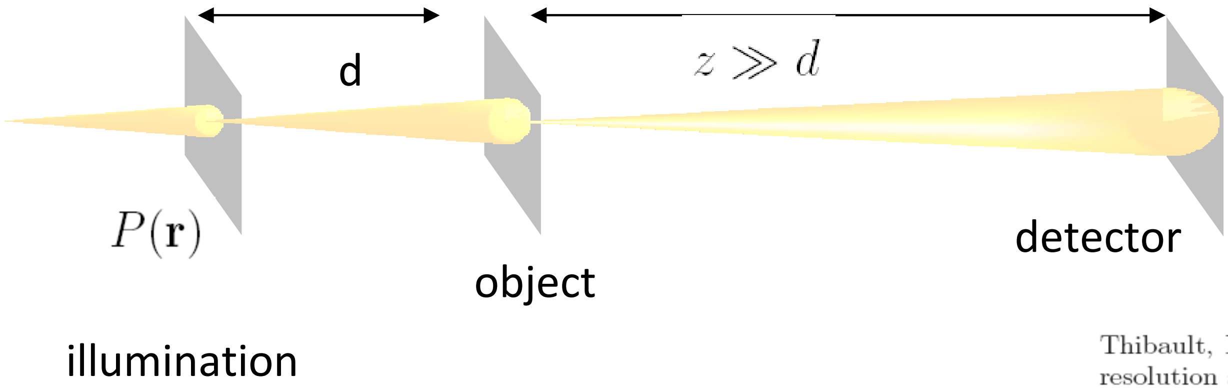

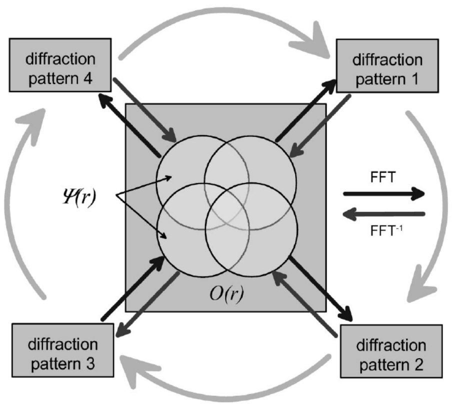

Thibault, P, Dierolf, M, Menzel, A, Bunk, O, David, C, and Pfeiffer, F High-resolution scanning X-ray diffraction microscopy. *Science* 321:379–382 (2008).

Ptychography - Principle

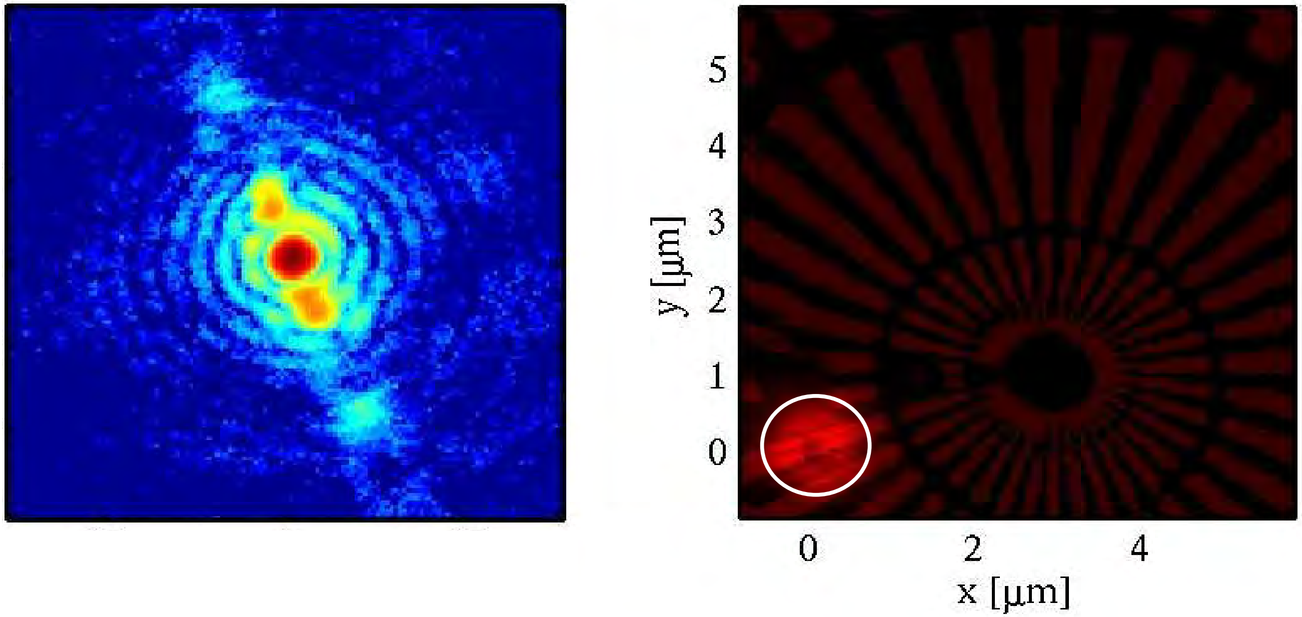

Ptychography - Principle

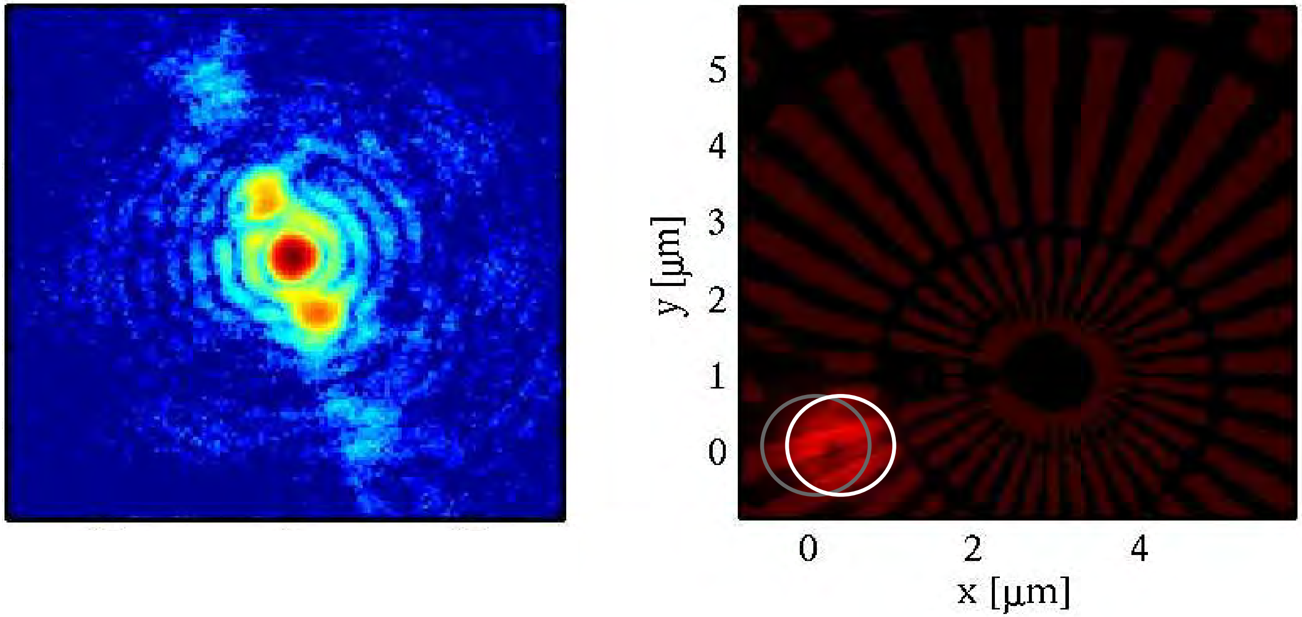

Ptychography - Principle

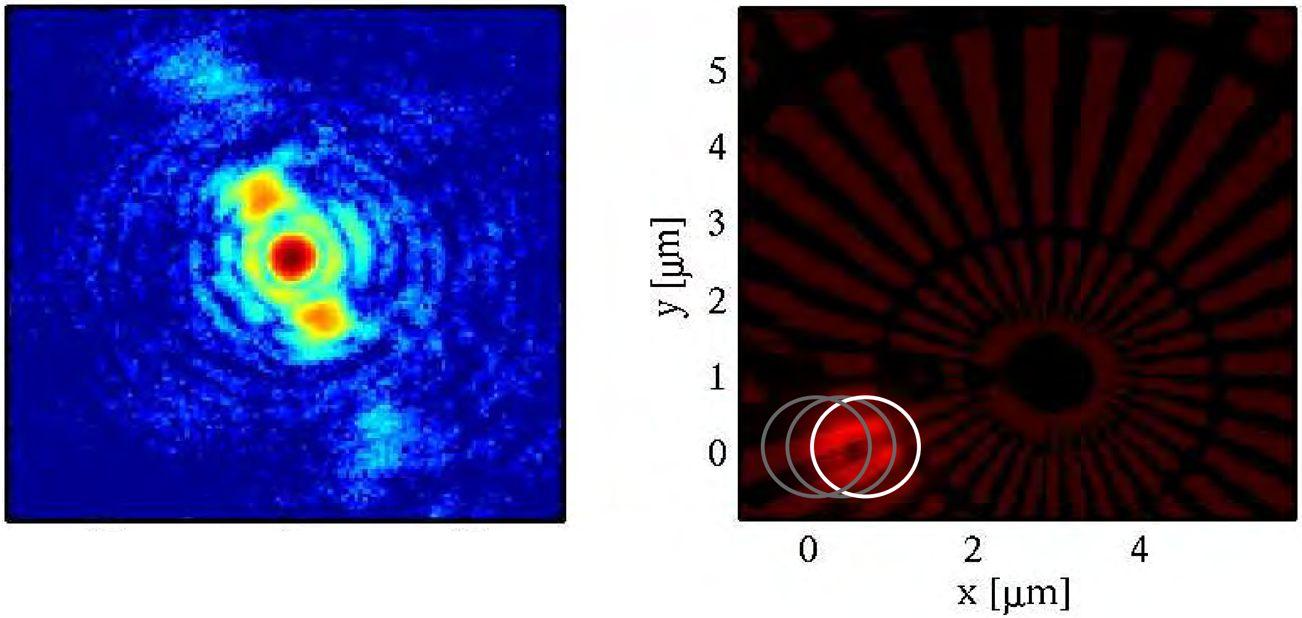

Klaus Giewekemeyer

DNA packing in nucleoids: *Deinococcus Radiodurans*

- **Among most radiationresistant organisms on earth, can survive 15 kGy of ionizing radiation**
- **Very effective DNA repair mechanism, DNA packing debated**

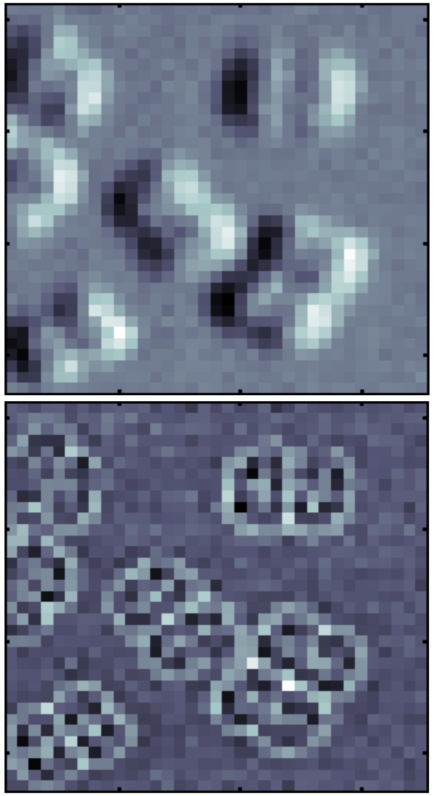

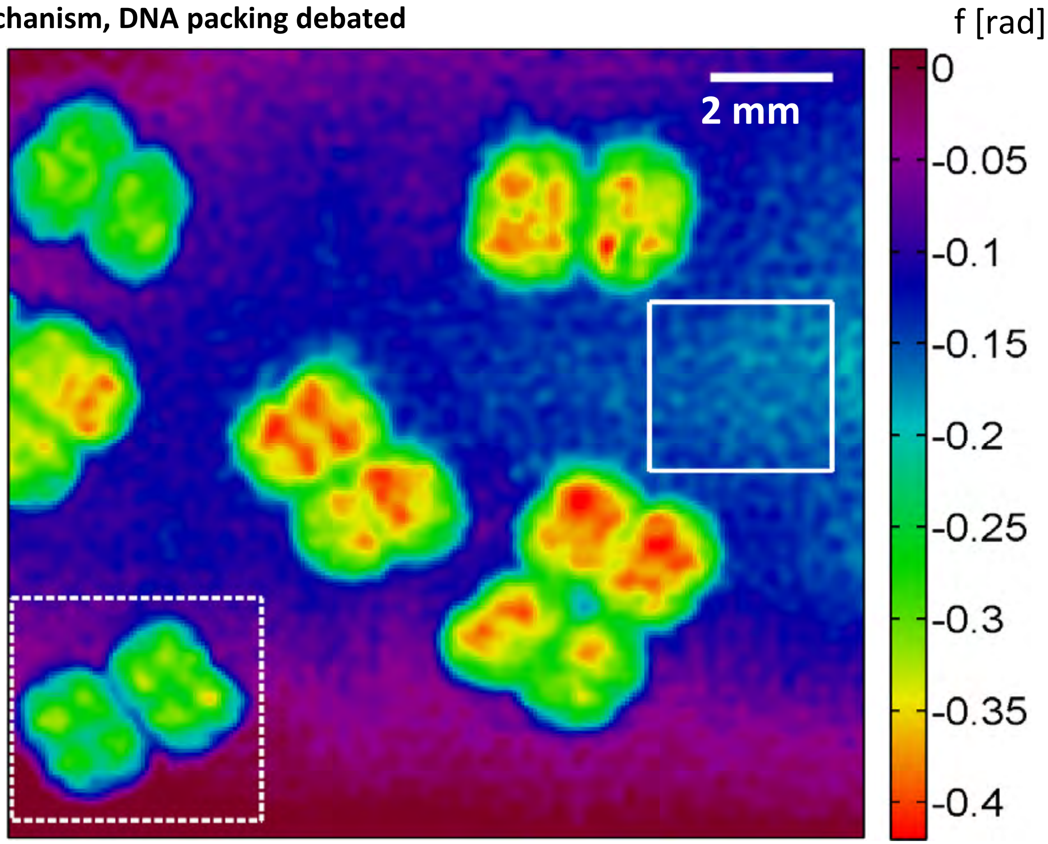

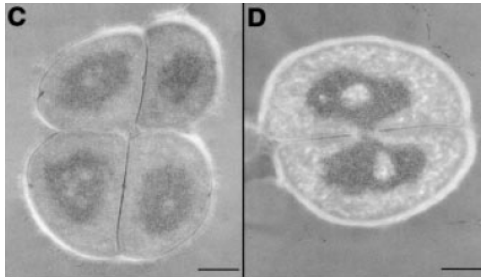

TEM-slices, Os-stained chromatin
Levin-Zaidman, Science (2003)

2x3 m size, tetrad morphology
4 identical copies of the genome

Left: Scanning X-ray Microscopy DPC / dark field

Right: super-resolution by phasing the coherent diffraction pattern

- Freeze-dried, unstained and unsliced cells
- Overall phase shift of single cell 0.25-0.3 rad (< 10% p), consistent with simulations
- 2500 iterations of SXDM algorithm, averaged over each 5th iterate, starting at 2000

Giewekemeyer *et al.*, PNAS (2010)

Far-field and near-field diffraction patterns !

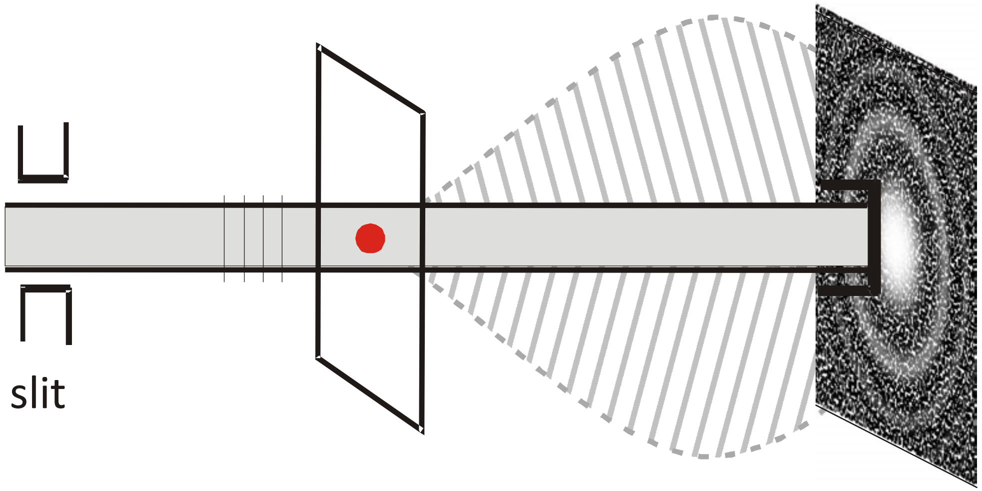

Missing low-q components

coherent farfield diffraction pattern

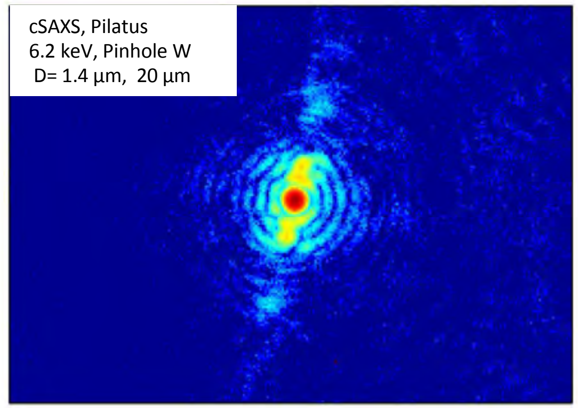

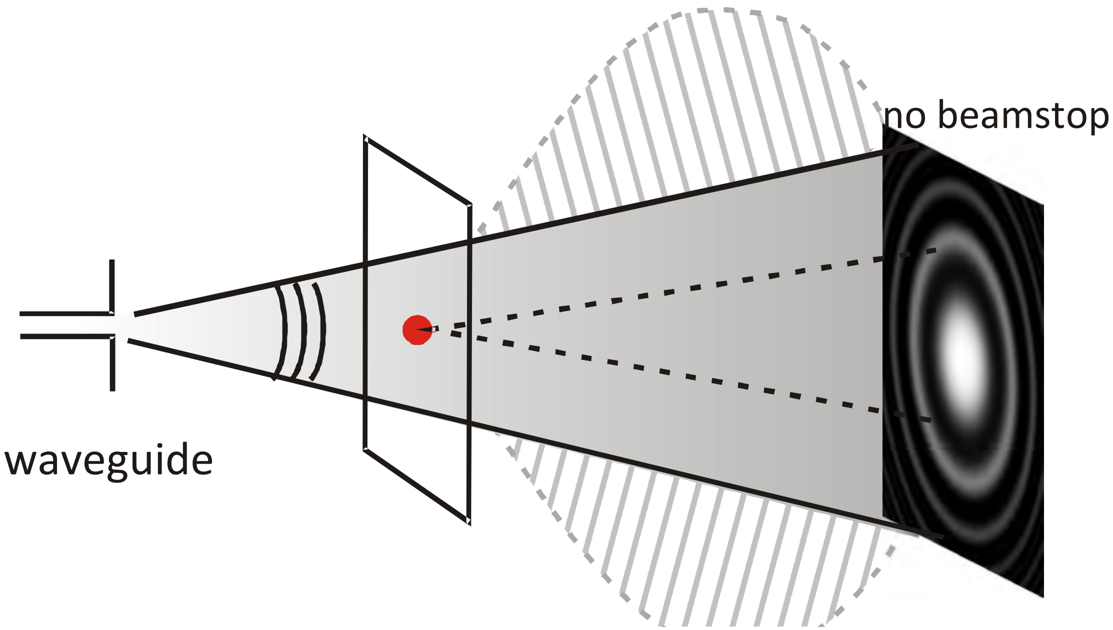

Fresnel diffraction pattern

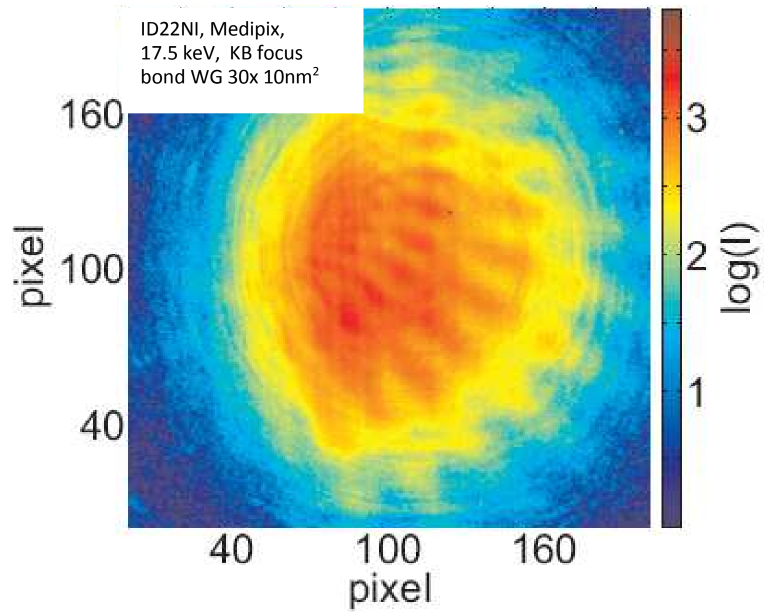

1.1 wave equations: a sequence of seperations

$$\nabla^2 \psi(\vec{r},t) + \frac{n^2(\vec{r})}{c^2} \partial_t^2 \psi = 0$$

$$\psi(\vec{r},t) = u(x,y,z) \exp(-i\omega t)$$

$$\nabla^2 u(x,y,z) + k^2 u = 0$$

$$u(x,z) = A(x,z) \exp(ik_0 z)$$

Parabolic wave equation

Ansatz

$$u(x,z) = A(x,z)\exp(ik_0 z)$$

insert in Helmholtz-Equation

$$\frac{\partial^2 A}{\partial x^2} + 2ik_0 \frac{\partial A}{\partial z} + \frac{\partial^2 A}{\partial z^2} + k_0^{\ 2}[n^2(x,z) - 1]A = 0$$

neglecting second order variation along optical axis

$$\frac{\partial^2 A}{\partial x^2} + 2ik_0 \frac{\partial A}{\partial z} + k_0^{\ 2}[n^2(x,z) - 1]A = 0$$

and in free space

$$\frac{\partial^2 A}{\partial x^2} + 2ik_0 \frac{\partial A}{\partial z} = 0$$

Justification of parabolic wave equation for small paraxial angles

plane wave in homogeneous media $$u(x,z) = u_0 \exp[i(k_x x + k_z z)]$$

with $k_x = nk_0 \sin\alpha$ and $k_z = nk_0 \cos\alpha$, we have

$$A(x,z) = u_0 \exp[ink_0(\sin\alpha)x]\exp[ik_0\{(n\cos\alpha) - 1\}z]$$

A(x,z) varys slowly with z ! For the derivatives

$$\frac{\partial^2 u}{\partial x^2} = -n^2 k_0{}^2 (\sin\alpha)^2 u = O(\alpha^2 k_0 u) = O(\delta k_0{}^2 u)$$

$$2ik_0 \frac{\partial A}{\partial z} = -2k_0{}^2 (n\cos\alpha - 1)A \approx -2nk_0{}^2((1-\delta)*(1-\frac{1}{2}\alpha^2) - 1)A = O(\delta k_0{}^2 A)$$

$$k_0{}^2 (n^2 - 1)A = k_0{}^2 (1 - 2\delta + \delta^2 - 1)u = O(\delta k_0{}^2 A)$$

$$\frac{\partial^2 u}{\partial z^2} = -k_0{}^2 (n\cos\alpha - 1)^2 u = O(\delta^2 k_0{}^2 A)$$

last term smaller by factor $\delta \ll 1$ and can be neglected

Kirchhoff diffraction integral

•derive diffraction integral (by use of Greens formula) from Helmholtz eq.

•Object plane z=0 with complex transmission $\tau(x,y)$

• illumination with plane wave, wavelength λ

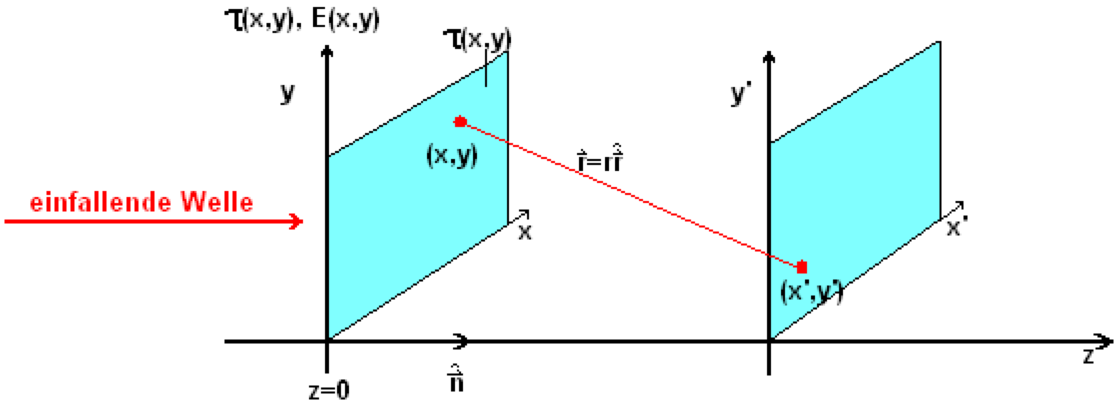

$$E(x',y',z) = \frac{1}{i\lambda} \int_{-\infty}^{\infty} \int_{-\infty}^{\infty} E(x,y) \frac{1}{r} \exp(ikr) \frac{1+\cos(\vec{n}\cdot\vec{r})}{2} dxdy$$

•Field in object plane $E(x,y)= \tau(x,y)E_i(x,y)$,

•Source point (x,y,0) emitts spherical wave (Huygens)

•Superposition of emitted waves E(x‘,y‘,z) in image plane

how the object comes in (Born approximation)

$$E_{out}(x,y) = E_{in}(x,y) \quad T(x,y)$$

$$T(x,y) = Exp[-k \int_{z\_object-\varepsilon}^{z\_object+\varepsilon} dz \, (\beta(x,y,z) + \mathrm{i}\,\delta(x,y,z))]$$

$$T(x,y) = \sqrt{T_{\mathrm{int}}(x,y)}\, e^{\mathrm{i}\varphi(x,y)} \quad T_{\mathrm{int}} = \left|T(x,y)\right|^2 \quad \varphi(x,y) = \arg T$$

paraxial approximation

$$\cos(\hat{n}\hat{r}) \approx 1$$

$$r = \sqrt{(x'-x)^2 + (y'-y)^2 + z^2} = z\sqrt{1 + \frac{(x'-x)^2}{z^2} + \frac{(y'-y)^2}{z^2}} \approx z + \frac{(x'-x)^2}{2z} + \frac{(y'-y)^2}{2z}$$

$$E(x',y',z) = \frac{\exp(ikz)}{i\lambda z}\iint E(x,y)\exp\left(\frac{ik}{2z}\left[(x'-x)^2 + (y'-y)^2\right]\right)dxdy$$

$$\frac{\exp(ikz)}{i\lambda z}\exp\left[i\frac{\pi}{\lambda z}(x'^2 + y'^2)\right] \quad \iint E(x,y)\exp\left(\frac{i\pi}{\lambda z}(x^2+y^2)\right)\exp\left[-2\pi i\left(\frac{x'}{\lambda z}x + \frac{y'}{\lambda z}y\right)\right]dxdy$$

$$C(x',y',z) \quad \iint E(x,y)\exp\left(\frac{i\pi}{\lambda z}(x^2+y^2)\right)\exp\left[-i\frac{2\pi}{\lambda}\left(\frac{x'}{z}x + \frac{y'}{z}y\right)\right]dxdy$$

$$C(x',y',z) \qquad FT\left[E(x,y)\exp\left[\frac{i\pi}{\lambda z}(x^2+y^2)\right]\right]\left(\frac{x'}{\lambda z},\frac{y'}{\lambda z}y\right)$$

$$\text{2D Fourier trans. in } \frac{x'}{\lambda z} \text{ and } \frac{y'}{\lambda z}$$

$$\iint E(x,y)\exp\left(\frac{i\pi}{\lambda z}(x^2+y^2)\right)\exp\left[i(q_x x + q_y y)\right]dxdy \qquad \left(q_x = \frac{2\pi}{\lambda}\tan\theta \approx \frac{2\pi}{\lambda}\frac{x'}{z}\right)$$

Fraunhofer approximation

$$E(x',y',z) = C(x',y',z) \quad \iint E(x,y) \exp\left(\frac{i\pi}{\lambda z}(x^2 + y^2)\right) \exp\left[i(q_x x + q_y y)\right] dxdy$$

for large distances compared to object $\quad x^2, y^2 << \lambda z \qquad$ (Fraunhofer diffraction)

$$E(x',y',z) = C(x',y',z) \quad \iint E(x,y) \; \exp\left[i(q_x x + q_y y)\right] dxdy$$

definition of Fresnel number : $F = a^2 / \lambda z$

size of object (aperture) : $\quad a$

Computation of the FK integral

$$E(x',y',z)=\frac{\exp(ikz)}{i\lambda z}\int\int E(x,y)\exp\left(\frac{ik}{2z}\left[(x'-x)^2+(y'-y)^2\right]\right)dxdy$$
$$\propto \quad E\otimes h_z$$

withFresnelpropagator

$$h_z(x,y)=\frac{\exp(ikz)}{i\lambda z}\exp\left(\frac{ik}{2z}(x^2+y^2)\right)$$

$$E(x',y',z)=FT^{-1}\left[FT[E(x,y)]\cdot FT[h_z(x,y)]\right]$$

$$FT[h_z(x,y)]=\exp(ikz)\exp\left(-i\pi\lambda z(\nu_x{}^2+\nu_y{}^2)\right)$$

alternatively

$$E' \quad \propto FT\left[E(x,y)\exp\left[\frac{i\pi}{\lambda z}(x^2+y^2)\right]\right]\left(\frac{x'}{\lambda z},\frac{y'}{\lambda z}y\right)$$

$$\text{2DFouriertrans.in}\frac{x'}{\lambda z}\text{and}\frac{y'}{\lambda z}$$

Propagation imaging

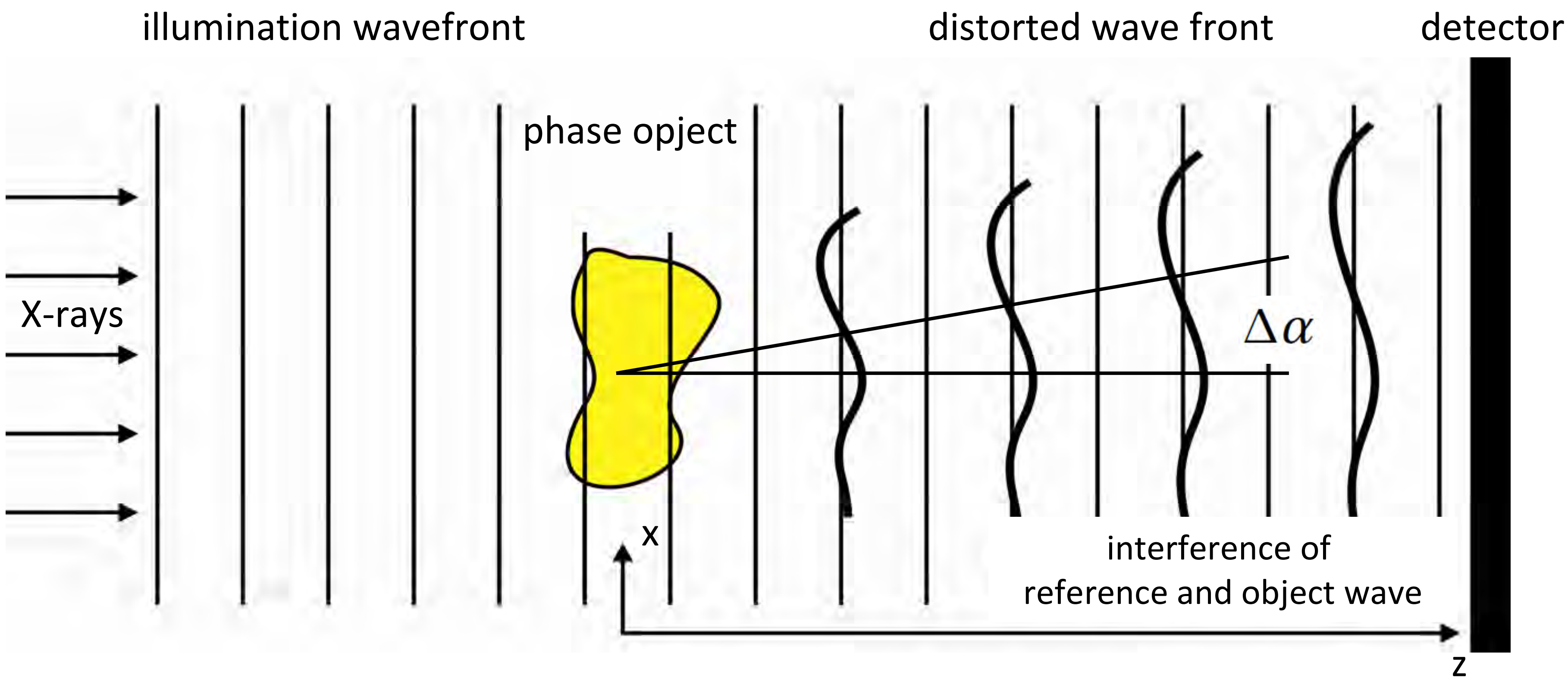

phase shift $\Delta\phi = k\,\Delta d\,(1-n)$

slab with index n

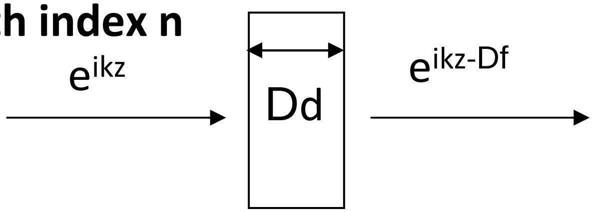

free space propagation

$$\Delta\alpha = \frac{\lambda}{2\pi}\frac{\partial\phi}{\partial x}$$

P. Cloetens et al. et al. ,1999; S.Wilkins et al. , 2000-2004

Imaging formation: Fresnel diffraction integrals

$$\psi(x',y',z) = \frac{1}{i\lambda}\int_{-\infty}^{\infty}\int_{-\infty}^{\infty}\psi(x,y,0)\frac{1}{r}\exp(ikr)\frac{1+\cos(\vec{n}\cdot\vec{r})}{2}dxdy \qquad \psi(x,y,0) = \psi_0\,\tau(x,y)$$

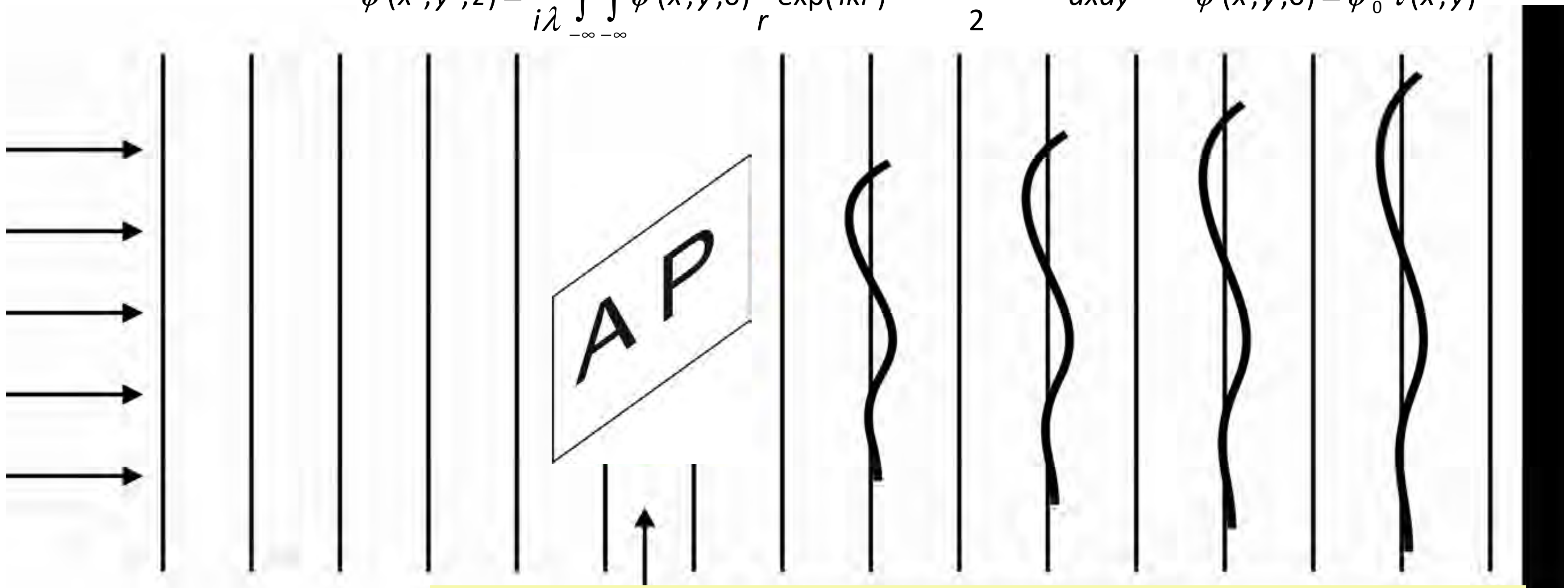

object with complex transmission function τ(x,y)

$$\psi(z) = FT^{-1}[\exp[iz\sqrt{k^2 - k_x^2 - k_y^2}]\;FT[\psi(0)]]$$

A P

Absorption Phase

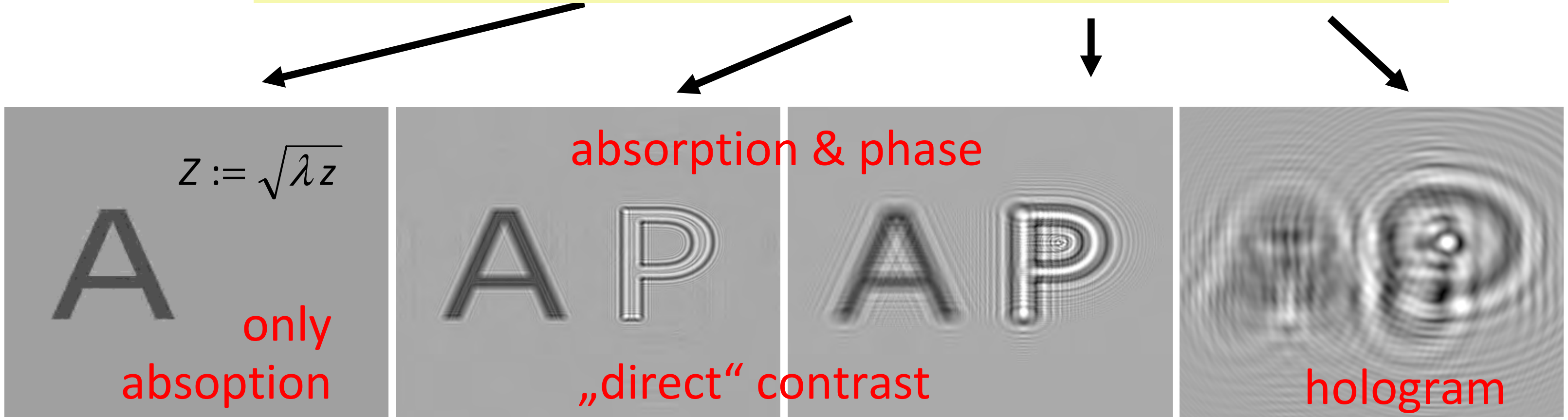

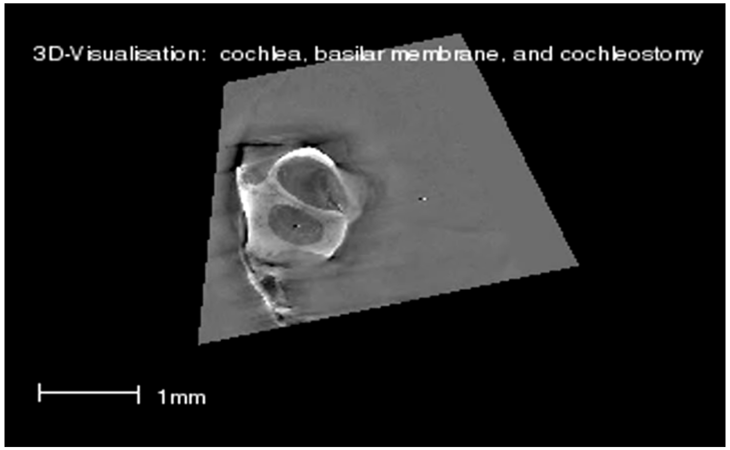

Density in 3D : resolution AND contrast matter !

Cochlea: Phase contrast vs. Absorption contrast

M.Bartels et al., unpublished

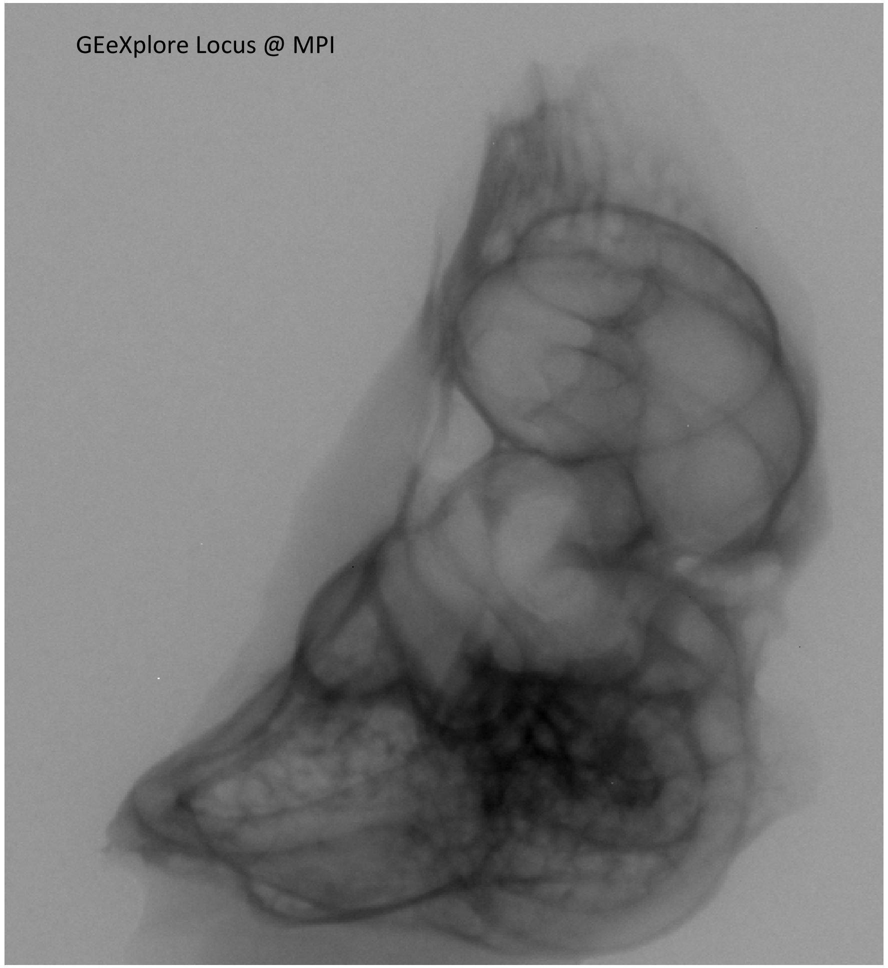

absorption versus phase contrast

$$n = 1 - \delta + i\beta$$

x-ray index of refraction

$$E_{out}(x,y) = E_{in}(x,y) \quad \tau(x,y)$$

$$\tau(x,y) = \exp[-k \int_{z}^{z+d} dz \, (\beta(x,y,z) + \mathrm{i}\,\delta(x,y,z))]$$

$\delta = 10^{-5} .. 10^{-9}$
$\beta = 10^{-7} .. 10^{-13}$

Absorption length μ

$$\beta = \frac{\mu}{2k}$$

Phase shift

$$\Delta\phi = k\,\Delta d(1-n)$$

slab with index n

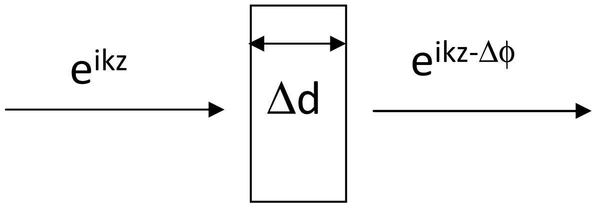

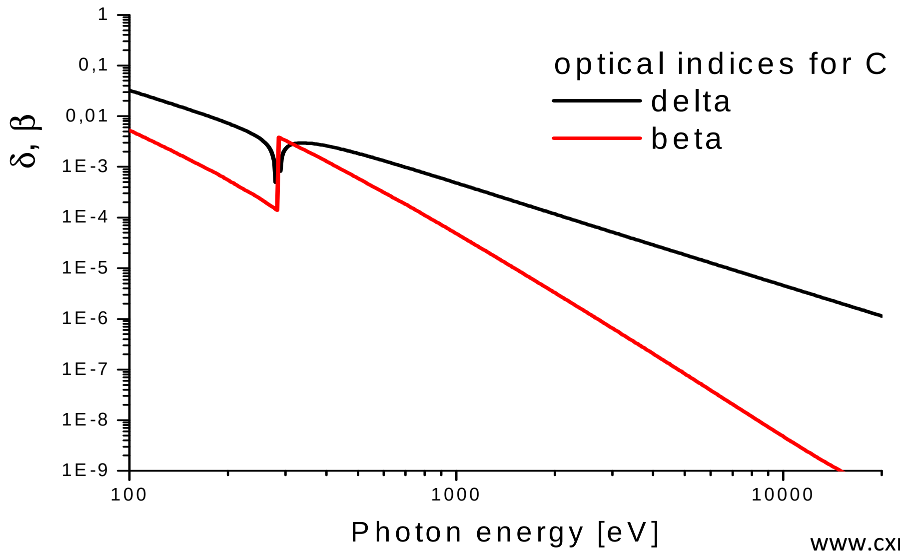

www.cxro.lbl.gov

δ >> b for low Z elements and high photon energies → phase contrast

weakly scattering object (Born approximation)

$$E_{out}(x,y) = E_{in}(x,y) \quad T(x,y)$$

$$T(x,y) = Exp[-k \int_{z}^{z+d} dz \, (\beta(x,y,z) + \mathrm{i}\,\delta(x,y,z))]$$

$$\tau(x,y) = \sqrt{\tau_{\mathrm{int}}(x,y)}\; e^{\mathrm{i}\varphi(x,y)} \quad \tau_{\mathrm{int}} = \left|\tau(x,y)\right|^{2} \quad \varphi(x,y) = \arg(\tau)$$

$$\tau(x,y) := Exp[\, i\ \delta(x,y)d - \mu(x,y)d/2 \,]$$

Contrast transfer function

$$f(x,y) = \exp(ikt) \times \underbrace{\exp[i\phi(x,y) - \mu(x,y)/2]}_{=\tau(x,y)}$$

complex object transmission function

$$\tau(x,y) = \exp[i\phi(x,y) - \mu(x,y)/2] \approx 1 + i\phi(x,y) - \mu(x,y)/2.$$

$$\tilde{E}_2(\nu_x,\nu_y) = \tilde{\tau}\tilde{h}_z \simeq (\delta_D(\nu_x,\nu_y) + i\tilde{\phi}(\nu_x,\nu_y) - \tilde{\mu}(\nu_x,\nu_y)/2)$$
$$\exp(ikz)\exp\left[-i\pi\lambda z({\nu_x}^2 + {\nu_y}^2)\right] \; ,$$

$$\tilde{I}(\nu_x,\nu_y) \approx \delta_D(\nu_x,\nu_y) + 2\tilde{\phi}(\nu_x,\nu_y)\sin\chi - \tilde{\mu}(\nu_x,\nu_y)\cos\chi$$

oscillatory CTF

$$\chi \;=\; \pi\lambda z({\nu_x}^2 + {\nu_y}^2)$$

dependence on spatial frequencies

Contrast transfer function (CTF)

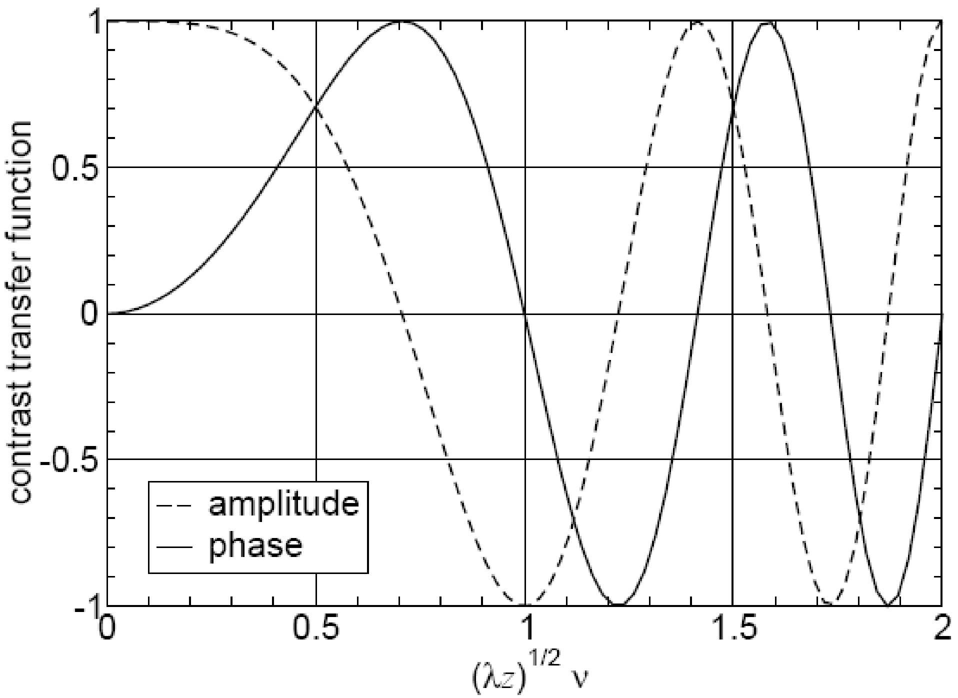

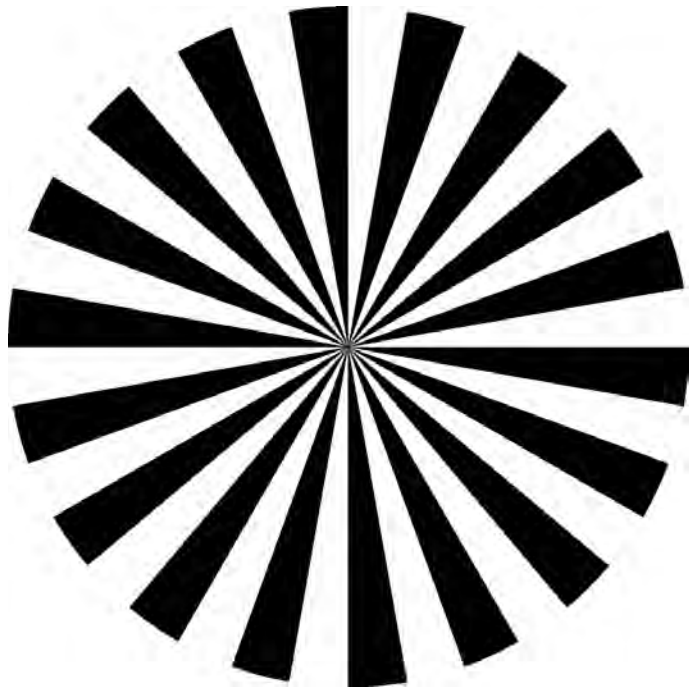

$$f(x,y) = \exp(ikt) \times \underbrace{\exp[i\phi(x,y) - \mu(x,y)/2]}_{=\tau(x,y)}$$

complex object transmission function

$$\tilde{I}(\nu_x,\nu_y) \approx \delta_D(\nu_x,\nu_y) + 2\tilde{\phi}(\nu_x,\nu_y)\sin\chi - \tilde{\mu}(\nu_x,\nu_y)\cos\chi$$

weak object approximation

$$\chi = \pi\lambda z({\nu_x}^2 + {\nu_y}^2)$$

-> oscillations as function of spatial frequencies

Fresnel scaling theorem:
an equivalence between parallel and point source illumination

$$n = 1 - \delta + i\beta$$

Phase shift

$$\Delta\phi = \delta k \, \Delta d$$

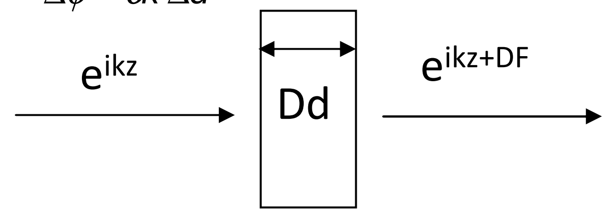

hologram recorded with the point source corresponds to a hologram recorded with a plane wave at an effective defocusing distance

$$Z_{eff} = \frac{z_1 z_2}{z_1 + z_2}$$

magnified by

$$M = \frac{z_1 + z_2}{z_1}$$

→magnification allows for a spatial resolution below detector pixel size!

→plane wave setup used for simulations and reconstruction

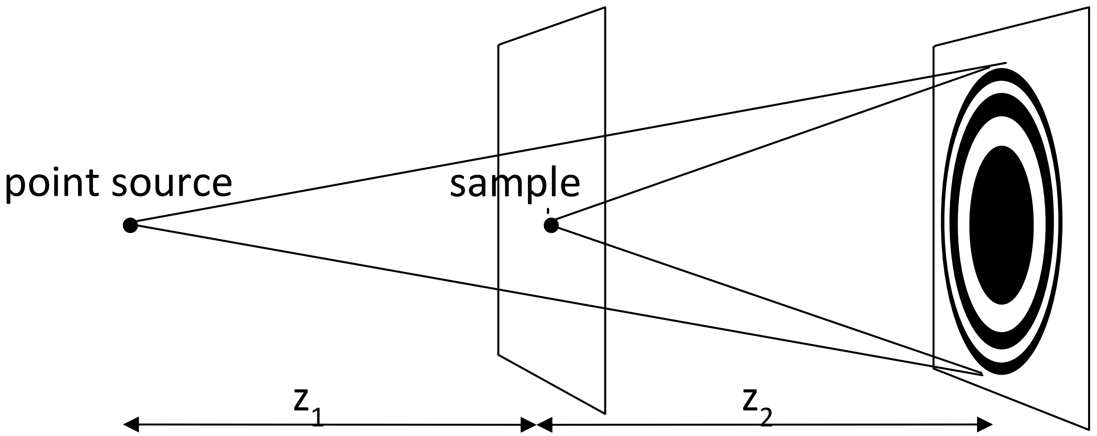

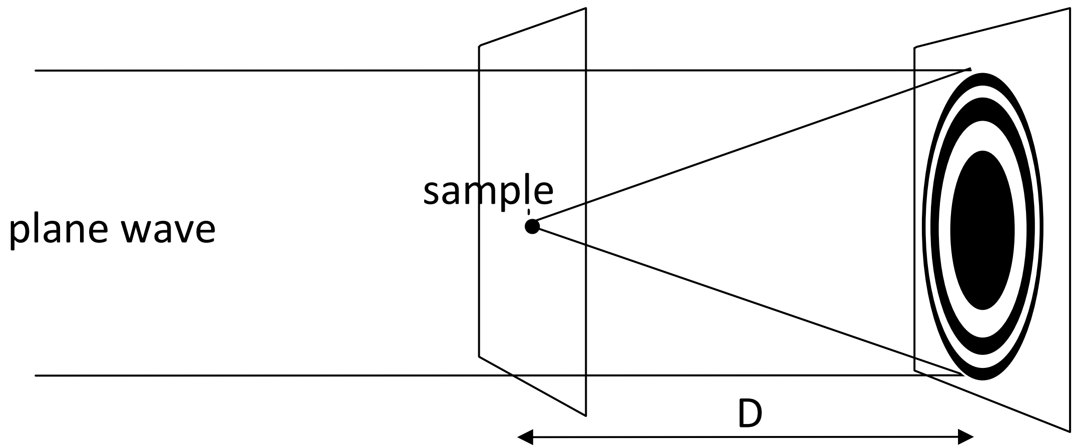

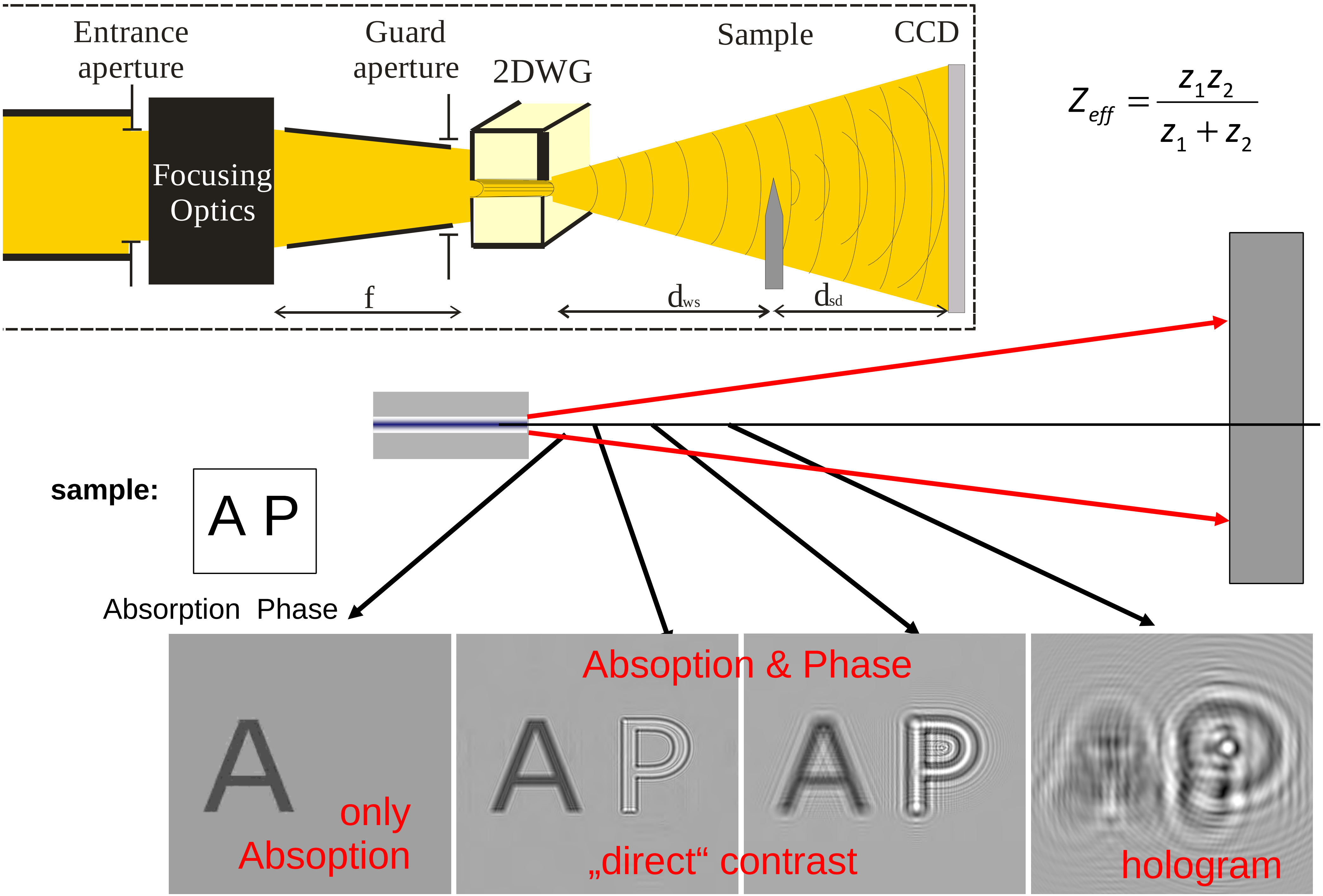
Entrance aperture
Guard aperture
2DWG
Sample
CCD
Focusing Optics
f
d_{ws}
d_{sd}
$Z_{eff} = \frac{z_1 z_2}{z_1 + z_2}$
sample:
A P
Absorption Phase
Absoption & Phase
only Absoption
„direct“ contrast
hologram

Zeros of phase contrast transfer (CTF): inversion of contrast

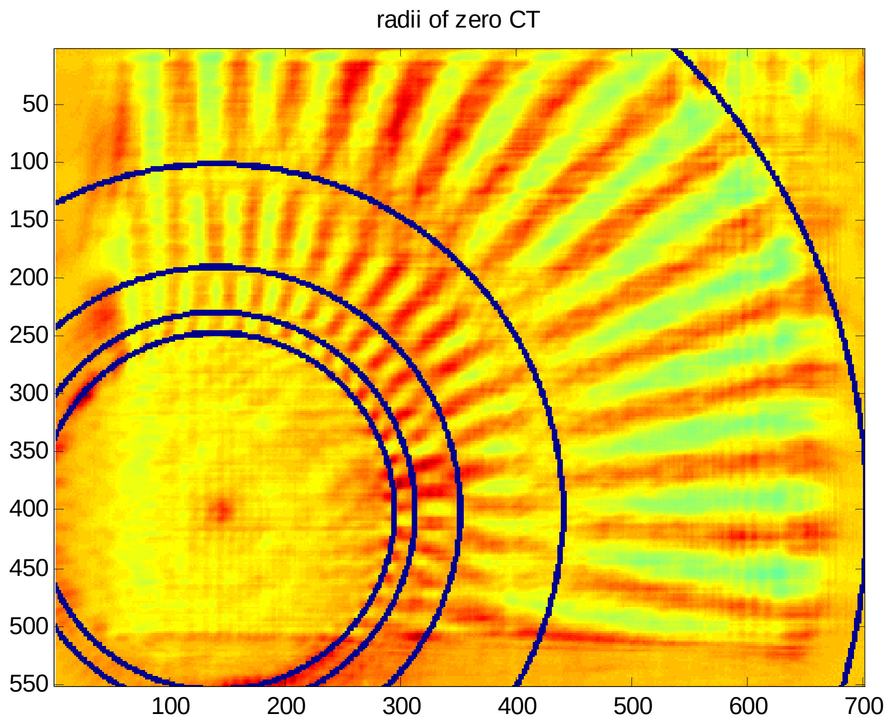

hologram of Siemens star
calibration pattern X50-30-2m, X-radia, h=180nm Au
ID22NI/ESRF, pink undulator beam, E=17.5 keV
Beam size: 146 x160 nm^2 10^{11} cps

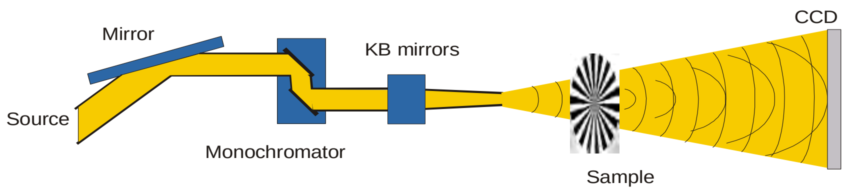

T. Salditt, K. Giewekemeyer, S. Krüger , R. Tucoulou, P. Cloetens, Physical Review B 2009

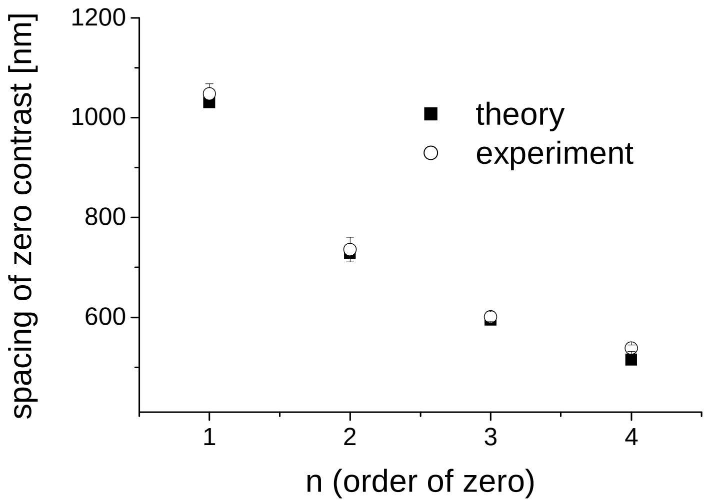

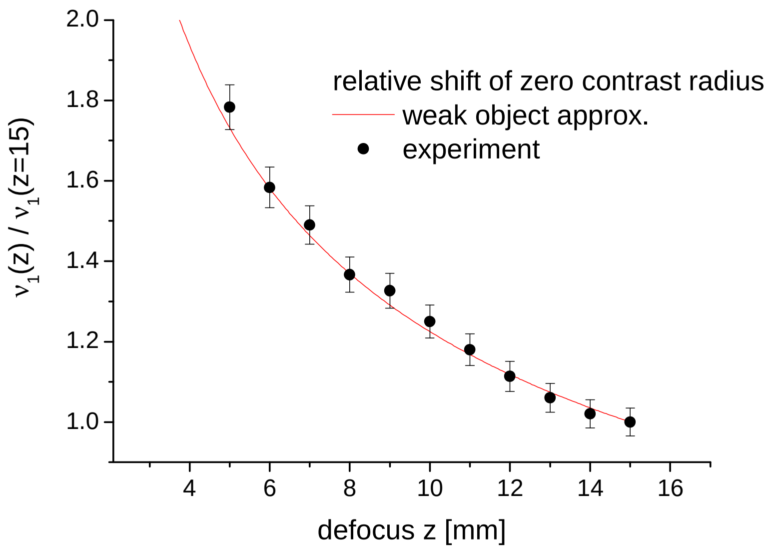

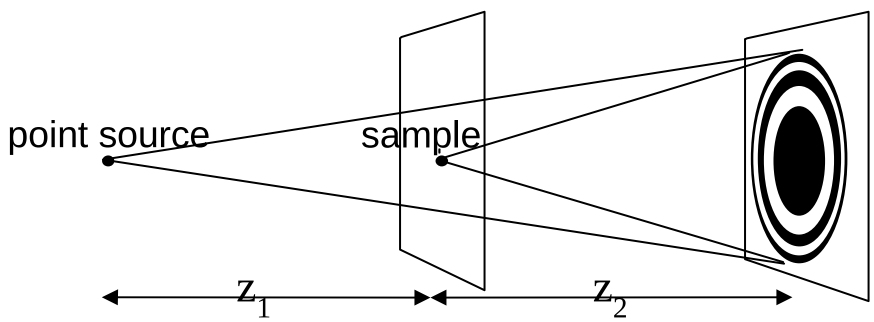

Nano-focused coherent x-ray beams for imaging …

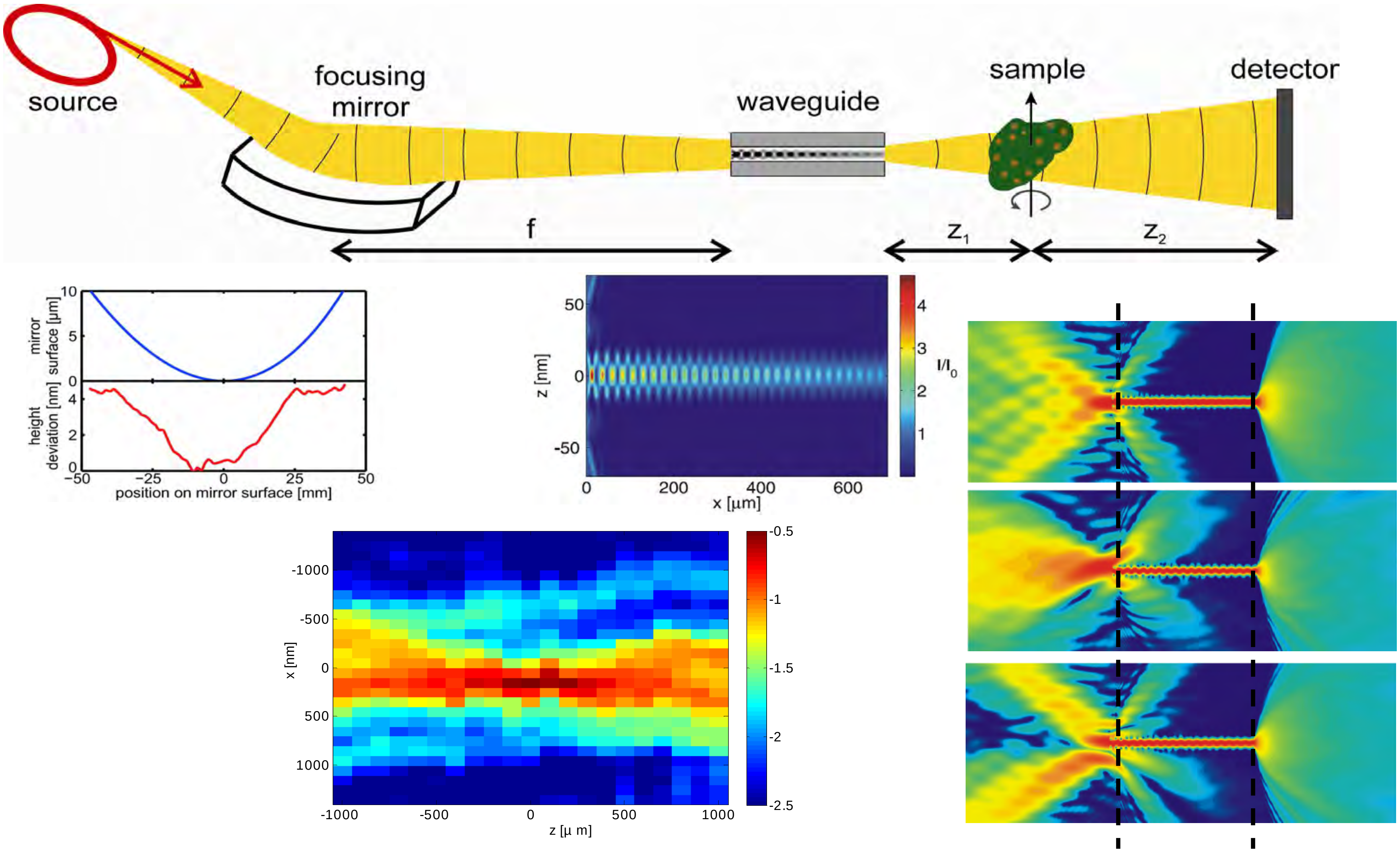

Improved algorithms for holographic imaging

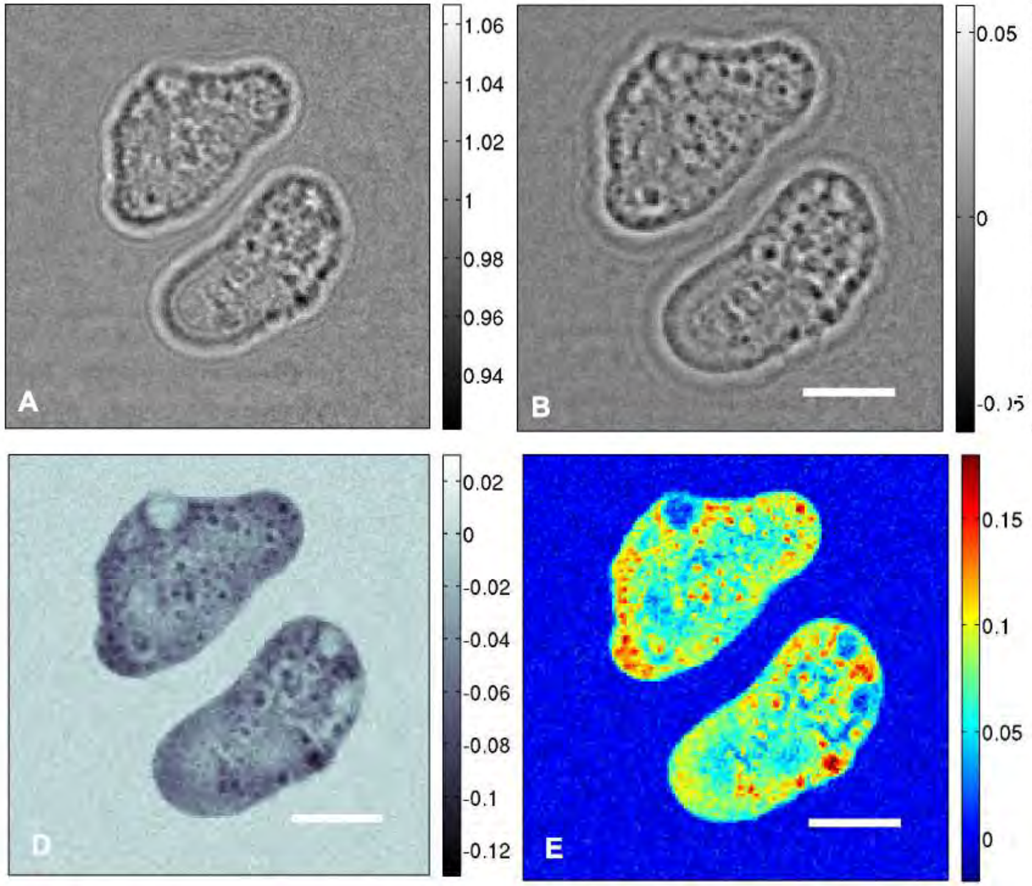

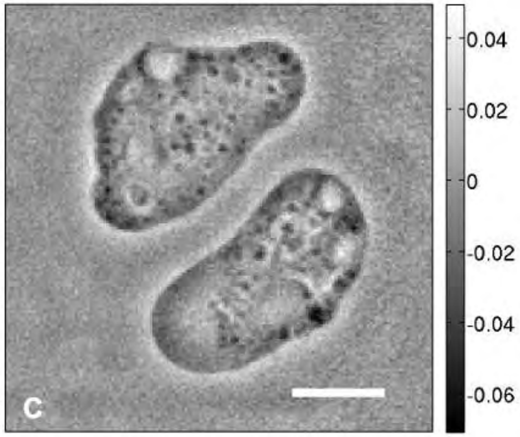

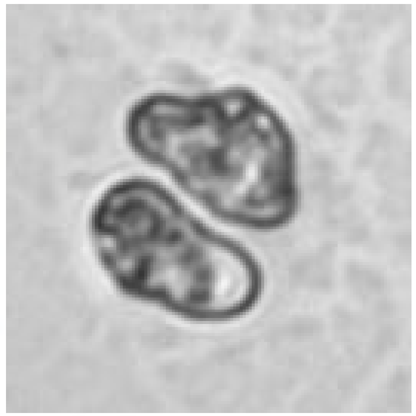

ID 22NI
35 x 35 nm crossed WG
17.5 keV
8.3 mm defocus

FIG. 2: Waveguide-based holographic diffraction imaging of *Dictyostelium Discoideum* cells. (A) Intensity hologram obtained from a sequence of 501 recorded images with and without the sample in the beam (for further details on experimental details see main text). (B) Single-step holographic reconstruction (phase) from hologram shown in A. (C) Iterative reconstruction of the object phase, obtained after 50 iterations of a standard Gerchberg-Saxton algorithm. (D) Quantitative phase reconstruction obtained with a modified Gerchberg-Saxton scheme, taking into accound the noise in the measured hologram and assuming a constant phase outside the cellular area (phase support). (D) Mass density distribution obtained from a rescaling of subfigure D. Scale bars denote 5 μm.

Giewekemeyer et al, PRA, 2011

transformation from spherical to parallel beam, z-> z_{eff}, M magnified coordinate system

$$I(x,y) = |D_{z_{\text{eff}}}[\psi_{\text{in}}\chi(x,y)]|^2 \simeq |\psi_{\text{in}} D_{z_{\text{eff}}}[\chi(x,y)]|^2$$

normalisation of the measured intensity I by empty beam

$$\bar{I}(x,y) \simeq |\psi_{\text{in}} D_{z_{\text{eff}}}[\chi(x,y)]|^2/|\psi_{\text{in}}|^2 = |D_{z_{\text{eff}}}[\chi(x,y)]|^2.$$

recording:

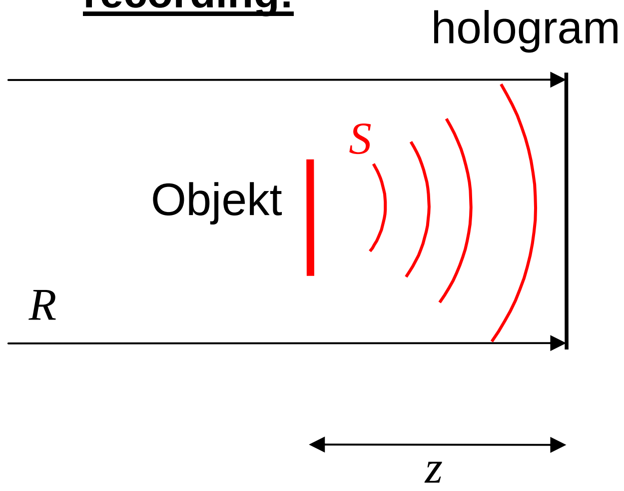

reconstruction:

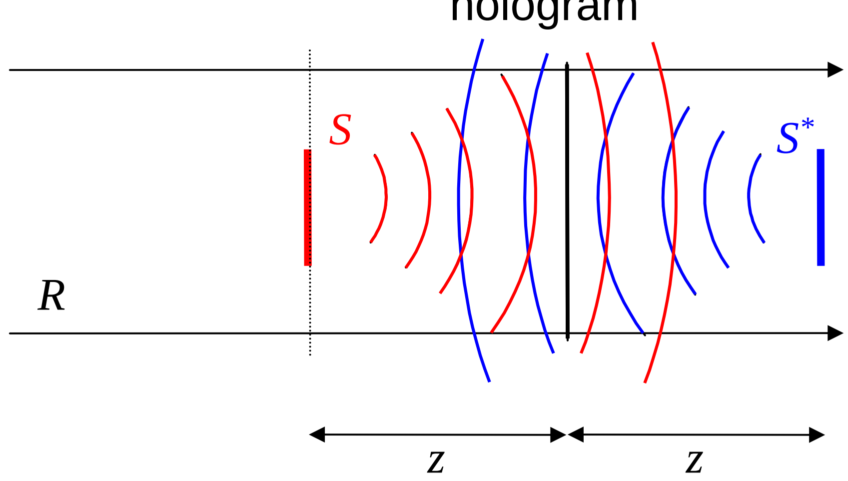

reference beam

signal

conjugated wave
„twin image“

$$\chi(x,y) = 1 + \tau(x,y)$$

$$\tau \xrightarrow{D_z} \tilde{\tau} = D_z[\tau]$$

$$I(x,y) \propto |1+\tilde{\tau}|^2 = 1 + \tilde{\tau} + \tilde{\tau}^* + |\tilde{\tau}|^2$$

$$\tau_{recon} = D_{-z}[1+\tilde{\tau}+\tilde{\tau}^*+|\tilde{\tau}|^2] = 1 + \tau + \tau^* + D_{-z}\left[|\tilde{\tau}|^2\right]$$

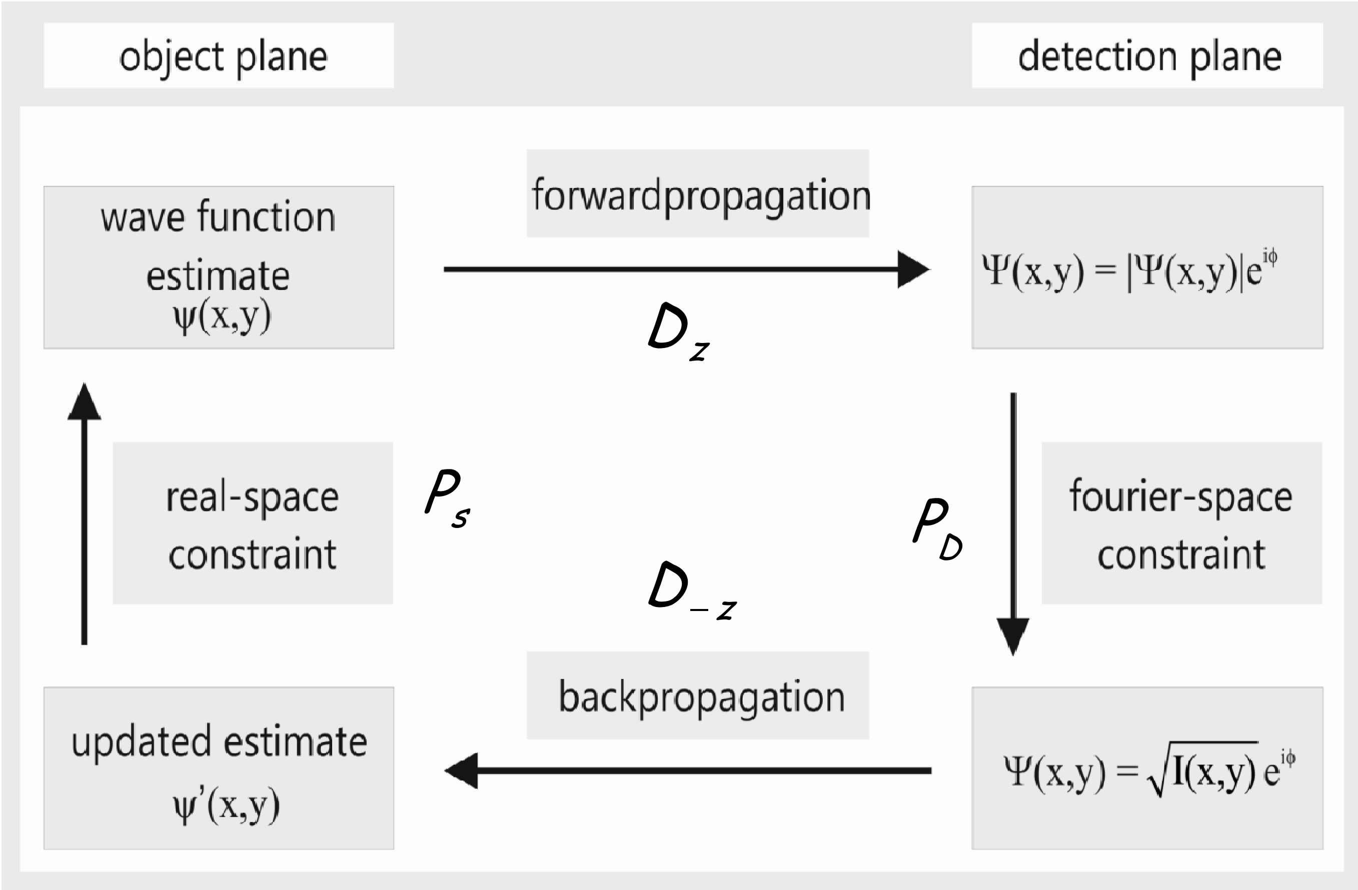

Propagator $D_z = FFT^{-1} \exp[\, iz\sqrt{k^2 - k_x^2 - k_y^2}\,]\, FFT$

P_D :'projector' in detector plane

$$|\tilde{\chi}'_n(x,y)|^2 = (1 - \frac{D}{d})\, \bar{I}(x,y) + \frac{D}{d}|\tilde{\chi}_n(x,y)|^2$$

$$d^2 = \frac{1}{N}\sum_{x,y}(|\tilde{\chi}_n(x,y)|^2 - \bar{I}(x,y)^2)^2$$

$D = \sqrt{2/<I_0>}$ noise

P_s : projector in sample plane

$$|\chi_{n+1}(x,y)| = |\chi_n(x,y)| - \beta(|\chi'_n(x,y) - 1|)$$

$$\arg(\chi_{n+1}(x,y)) = \begin{cases} \arg(\chi_n) - \gamma \arg(\chi'_n) & \forall (x,y) \notin S \\ \min(\arg(\chi'_n, 0) & \forall (x,y) \in S \end{cases}$$

S support (from holographic reconstruction)

Non destructive imaging ?

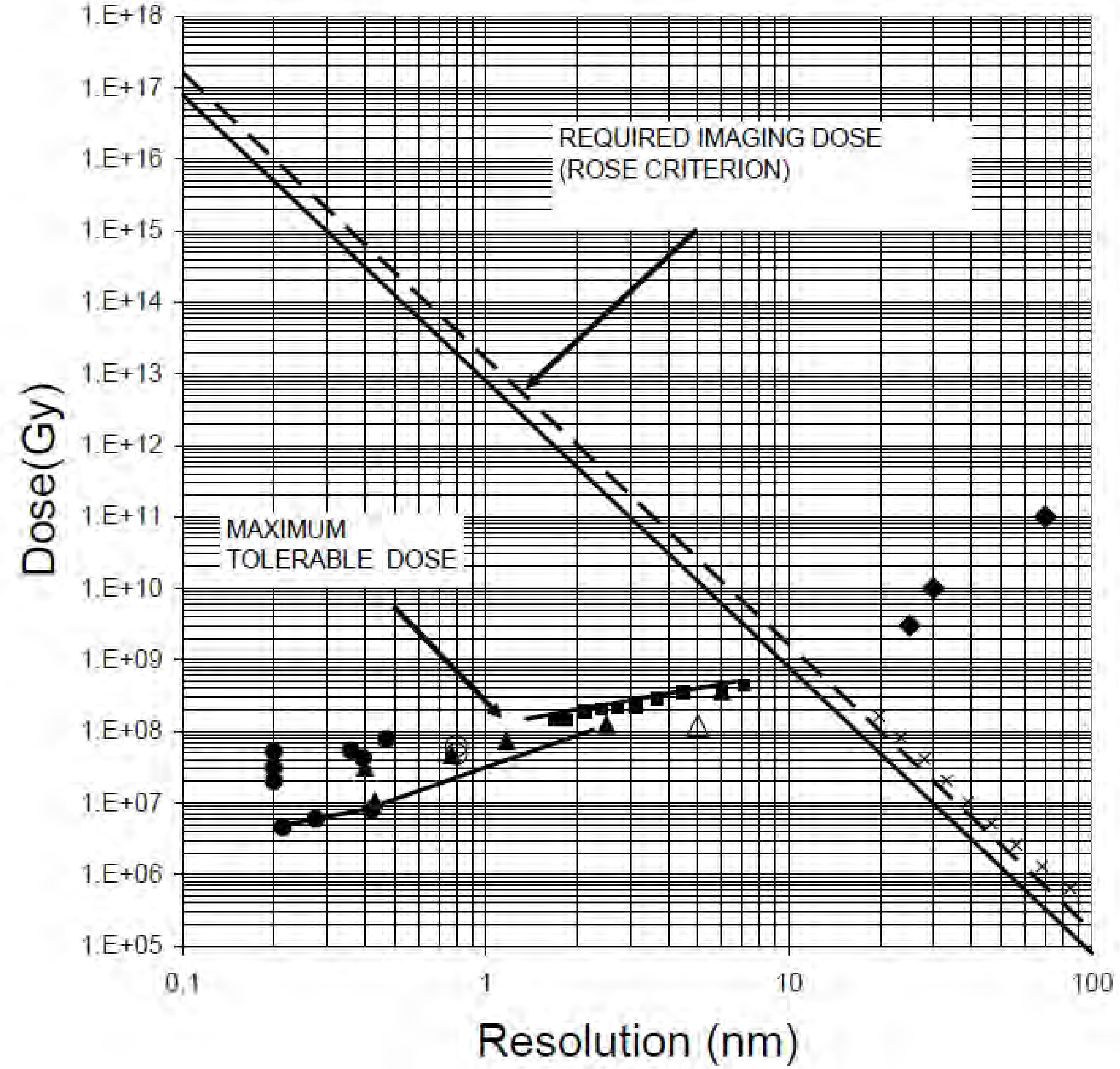

Howells et al., 2009

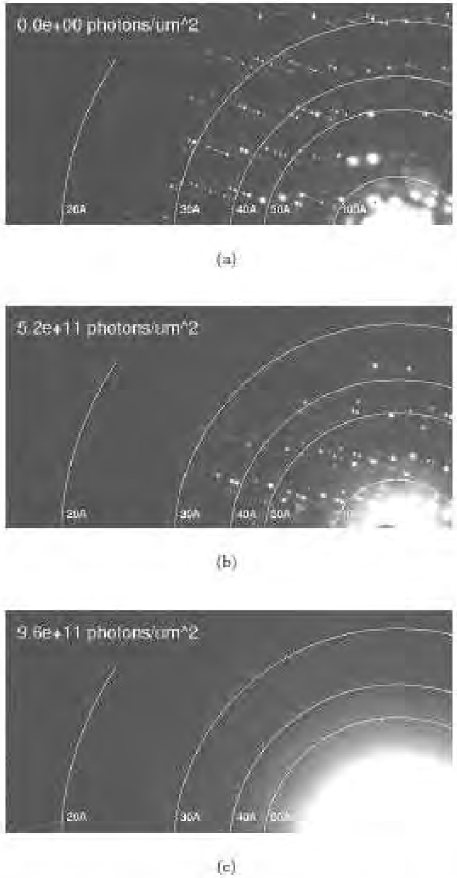

FIG. 3: Three spot patterns from the series described in the text recorded from the ribosome crystal. Many of

$$D = \frac{\mu\, P\, h\nu}{\varepsilon\, \sigma_s} = \frac{\mu\, P\, h\nu}{\varepsilon}\, \frac{1}{r_e^2\, \lambda^2\, |\rho|^2\, d^4},$$

$$N_0 = \frac{P}{r_e^2\, \lambda^2\, |\rho|^2\, d^4}.$$

credentials / acknowledgements

Original work:
Klaus Giewekemeier, R. Wilke *cells, coherent imaging, image reconstruction*
Andre Beerlink Michael Mell *Fresnel imaging of membranes*
Sebastian Kalbfleisch, Matthias Bartels *holography, propagation imaging tomography*
Henrike Neubauer, Sven Krüger *waveguide optics and fabrication*
Markus Osterhoff *numerical optics, focusing, mirror design*
Marius Priebe *cellular nanodiffraction, microliquid jet*
Simon Castorph, Sajal Ghosh, Sebastian Aeffner *synaptic vesicles, fusion intermediates*
Tanja Ducic, Christian Oldendrowitz *imaging of neural cells and tissues*
Don-Du Mai, Jörg Hallmann, Tobias Reusch *FLASH experiments, lipid membranes*

S. Köster, Institut für Röntgenphysik
M. Holt, R. Jahn MPI biophys. Chemie Göttingen

M. Sprung, HASYLAB/DESY, P. Cloetens ESRF Grenoble, F. Pfeiffer, P. Thiebault, C. Kewish Swiss Light Source Villigen , SFB755 *Nanoscale Photonic Imaging,* SFB 803*,* SFB 937*,* BMBF, VI Helmholtz

Graphics: I am endebted to Christoph Ollinger, Christian Fuhse, Sven Krüger, Andre Beerlink, Klaus Giewekemeyer and many other of my team members for graphics.